PERFORMANCE ANALYSIS OF SMALL FORMAT AERIAL PHOTOGRAPHY (SFAP) IN ASSESSING CURRENT STATUS AND TRENDS IN WIND EROSION

A Case Study in the Longonot-Kijabe Hill area, Naivasha District, Kenya

A. Nagelhout
February, 2001

PERFORMANCE ANALYSIS OF SMALL FORMAT AERIAL PHOTOGRAPHY (SFAP) IN ASSESSING CURRENT STATUS AND TRENDS IN WIND EROSION

A Case Study in the Longonot-Kijabe Hill area, Naivasha District, Kenya

by

A. Nagelhout

Thesis submitted to the International Institute for Aerospace Survey and Earth Sciences in partial fulfilment of the requirements for the degree of Master of Science in Geoinformation Science and Earth Observation, with specialization in Soil Information Systems.

Degree Assessment Board

Assoc. Prof. Dr Rossiter	(Head of Division)
Prof. Dr. A.K. Skidmore	(Extern. examiner)
Drs P. Hofstee	(Internal Examiner)
Ir G.R. Hennemann	(Main supervisor)
Mr J.A. Horn M.Phil.	(2^{nd} supervisor)
Dr. A. Farshad	(Student Advisor)

INTERNATIONAL INSTITUTE FOR AEROSPACE SURVEY AND EARTH SCIENCES
ENSCHEDE, THE NETHERLANDS

Disclaimer

ABSTRACT

This study is directed to assess the current status and trend in wind erosion in the Lake Naivasha area, Kenya.

In the last decade dramatic changes have occurred in the Longonot-Kijabe Hill area, where land degradation, especially wind erosion has altered the landscape. Although several satellite images (Landsat) were taken of this area, the resolution of these images is too low to assess the current status of wind erosion in the study area. Aerial photographs are available, but 9 years old, just taken at the start of the wind erosion process.

Small Format Aerial Photography in combination with GPS is a low cost technology, with rapid results, an excellent tool to obtain actual photographs of the study area. With a hired Cessna 182 and a Minolta X300 camera (35mm) 130 photographs were made, covering the reconnaissance area with 5 flightlines. 28 photographs were selected which covered the study area. These photographs were rectified (projective transformation) with GPS observations made in the field.

During fieldwork a soil survey was carried out to obtain general soil information of the area and information about the Wind Erosion Features was annotated.

The conventional aerial photographs of 1991 were interpreted and resulted into three maps, geopedological map, land use map and status of land degradation 1991. Also the SFAP's were interpreted, giving the current status of land degradation and land use in the study area. With these maps of two different periods, trends and rate of land degradation for the period 1991-2000 was calculated.

A severity classification of the current land degradation situation in the study area was created, following the guidelines of the GLASOD methodology, adapted to the study area.

An analysis was made to the underlying factors of wind erosion in the area. The micro-relief and soil properties play an important role. One map unit in the Volcanic Plain consists of several low dunes, where a Bw-horizon with a low erodibility covers highly erodible dark grey sand layers. Destroying the Bw-horizon in this particular map unit will start the wind erosion process.

The agricultural function of the area has reduced significantly in these 9 years. Several complexes of deflation trenches are found on abandoned fields which were under agricultural practices 9 years ago.

Acknowledgements

At the completion of this thesis it is a pleasant duty to express my gratitude to those who were involved in my professional training at ITC and those who co-operated in this study, especially the Soil Science Division.

I am very grateful to Ir. G.R. Hennemann for his assistance both in the field and thesis writing.

I would like to thank J.A. Horn M.Phil, my second supervisor, for his constructive comments about the flight preparation.

Also many thanks to Angus Simpson and his wife, for their willingness to let fly me without a door above the area and for their hospitality. After such a flight, a lunch with them is like heaven on earth!

I would like also to give my thanks to Drs. R. Becht and Ing. R. Dost for their assistance in the field and for the organisation of our stay in Naivasha.

Thanks also to J. Hendrikse and Dipl. Ing. K. Grabmaier, for their interest and advice with respect to rectifying the Small Format Aerial Photographs.

My course mates, Paul, Tilaya, Rana, Hoang, Atkilt and Fabiola, I always enjoyed their company.

Table of content

1 Introduction

1.1 Background and problem statement

Natural resource development projects are more and more making use of Geographical Information Systems (GIS). But for many projects the access to data is limited. Generally there are topographic maps, but other maps like soil maps, geomorphologic maps or geological maps are scarce. And when present they do not always comply with the requirements. For those projects without spatial information it will be difficult to assess, for example:

- Land use/cover changes
- Land degradation
- Rural/urban settlements
- Disaster scenes

Personal experience of the author in a watershed management project without actual information of land degradation and land cover made it difficult to apply a GIS as a management tool. Because of lack of actual information at the start of the project, an evaluation of project activities could not be met. For monitoring and evaluation, actual spatial data can contribute to review project activities in an objective way.

For short or medium term projects actual spatial data has to be obtained as soon as possible because of time constraints. In case of disasters, like mudflows, flooding and earthquakes, up to date information is essential. Large scale photographs, obtained in a short time do have the advantage of analysing recent changes and give more information about patterns of limited size, such as in land degradation.

In general there are two aerospace data sources generally involved in geographical data acquisition:

- ❑ Satellite images
- ❑ Aerial Photographs (AP's)

Satellite images cover large areas, which for some project will not be necessary. Furthermore they are costly, and do need experienced technicians to handle the data. Although the resolution (and price) of new satellites is increasing, the classical satellite images (Landsat and SPOT) are relatively poor to determine certain objects. Delivery time can be long.

AP's are an excellent source for large-scale spatial data for natural resource specialist. Depending of the scale various objects can be mapped into a higher or lower detail. To obtain AP's costs and delivery time are important factors to be considered. For example for urban planning in Indonesia there was a need to update the maps each year, but large format material and general town maps were produced in 3 to 5 years, which could not meet the requirements for town planners (Warner, Graham et al. 1996).

In most countries AP's do exist, but:

1. May not be recent.
   Especially when there have been changes in land use, land degradation or immigration, old AP's can not give up-to-date and correct information.
2. Do not have the appropriate scale
   There are AP's, but not with the appropriate scale. Most AP's have a scale of 1:20.000 to 1:60.000, and AP's with a scale higher than 1:10.000 are needed.
3. Although having the appropriate scale, are only available for of 1 moment.
   For monitoring reasons, AP's of different time moments are needed (for example seasonal change analysis).

As mentioned before money is in general the limiting factor for obtaining actual spatial data. As most projects do not have a budget to obtain this information, other ways have to be analysed. Small Format Aerial Photography could be an alternative to provide actual data. Recent developments with GPS have provided additional support for SFAP and together they form an economic concept with great promise for future mapping (Heimes, Poole et al. 1993).

1.2 Research problem

On the south-eastern side of Lake Naivasha, Kenya, the Longonot-Kijabe Hill area is facing a severe The Longonot-Kijabe Hill area which is located just south-east of Lack Naivasha in Kenya, is currently suffering from severe wind erosion. An important constraint to the proper analysis of the wind erosion problems is the general lack of up-to-date information about the area.

This constraint includes the total absence of recent aerial photographs from the area. The most recent AP's are from 1991 but the land degradation problems as a result of wind erosion started only after 1995. Satellite images are available for 1989, 1995 and 2000 (TM-Landsat) but they generally have too low a resolution for the analysis of wind erosion features. Under such circumstances there appears to be clear need for applying Small Format Aerial Photography (SFAP) - partly in complementary use with conventional aerial photography - to analyse and assess above wind erosion problems.

1.3 Objectives

The main research objective is:

- To use and analyse Small Format Aerial Photographs (SFAP) as complementary to conventional aerial photography to assess the current status, and trends in wind erosion.

The specific objectives are:
Through complementary use of SFAP and conventional aerial photographs:

1. To analyse, map and assess current spatial extent, severity of wind erosion.
2. To analyse, map and assess current trend and rate of wind erosion induced land degradation
3. To analyse existing relationships between current wind erosion status and wind erosion trends with underlying erosion factors in the area.

To assess above output on the basis of

1. Geometric accuracy
2. Thematic accuracy
3. Resource and cost efficiency

1.4 Hypotheses

Georeferenced SFAP's are an adequate complement for assessing current status and trends of land degradation for small (pilot) areas.

1.5 Research questions

1. What geometric accuracy and image quality is needed to accurately map land degradation at a scale of 1:5000?
2. What are the differences using different methods for geometrically correction of aerial photographs and SFAP?
3. Are the operational aspects like cost, time and required user expertise significant different than the "conventional" way?
4. What are the underlying factors of wind erosion in the area?
5. What is the trend or rate of erosion in the area
6. How severe is the situation and can features be classified in severity classes?

7.

1 Literature review

1.1 Land degradation

1.1.1 Wind erosion

Land degradation including wind erosion is a major environmental concern of modern times. However, the general effects of land degradation on the environment are easily exaggerated when factual information is scarce. Despite the voluminous literature on the global, regional and national problems of land degradation, reliable quantitative data on the magnitude of the problem is often scarce.

Removal or depletion of vegetation or vegetative residues that protect the land facilitates erosion of soil by wind. Wind erosion may occur in areas where climatic, soil and vegetative conditions are conducive. Such conditions include the following:

- Loose, dry and finely divided soil;
- Sparse or absent vegetative cover with some smooth soil surface;
- A sufficient large field; and
- Sufficiently strong wind to initiate soil movement.

Some humid and sub-humid areas are affected, but a combination of the above conditions is more common in arid and semi-arid areas.

Excessive or untimely tillage, inappropriate implements, burning of crop residues and excessive livestock grazing all contribute to erosion on cultivated land. On pasturelands, the dominant causes have been overgrazing and inadequate animal management during grazing. In rangelands where pastoralism is practised, the quality of pastures subject to excessive grazing during dry periods deteriorates, the proportion of edible perennial plants decreases, and the proportion of annuals increases.

The thinning and death of vegetation during dry seasons or droughts increase the extent of bare ground and deterioration in surface-soil conditions. This increases the fraction of erodible aggregates on the soil surface. In rainfed farming areas, removal of the original vegetation exposes the soil to accelerated wind and water erosion. Soil erodibility, which is susceptibility or ease of detachment and transport by wind, has been recognised for many years now as being the primary variable affecting wind erosion. Wind removes from the field the most fertile portion of the soil, and therefore, lowers land productivity. Some soil from damaged land becomes suspended as part of the atmospheric dust. Atmospheric dust obscures visibility and pollutes the air. Blowing soil also fill road ditches, reduces seedling survival and growth, and increases the susceptibility of plants to certain types of stress, including diseases.

The arid and semi-arid lands of Kenya cover more than 80% of the country. These lands are characterised by low and unreliable rainfall whose seasonal distribution is also very erratic. In such areas, soil erosion by wind is a serious menace, which is accelerated by the ongoing depletion of vegetation cover due to opening up farming activities in areas with fragile ecosystems as well as by overgrazing (Karanja 1997). Above also applies to the sub-humid parts of Kenya such as the central part of the Rift Valley in which the study area is located.

1.1.2 Models to predict wind erosion

The Wind Erosion Equation (WEQ) and its successor the Revised Wind Erosion Equation (RWEQ) have been the primary wind erosion prediction equations currently in use. The WEQ is described by the functional relationship:

$$E=f(I,C,K,L,V)$$

where

E is the potential average annual soil loss in tons per acre per year;

I is the soil erodibility in tons per acre per year determined by the amount of aggregates larger than 0.84 mm in diameter;

C is the climatic factor, based on wind erosivity with reference to the climate at a standard location (Garden City, Kansas);

K is the soil roughness, expressed in terms of the height of standard ridges;

L is the field with, maximum unsheltered distance across the field along the direction of the prevailing wind; and

V is the vegetation cover factor, expressed in relation to an equivalent quantity of flat small grain stubble.

The WEQ and RWEQ have been developed and used largely in the USA, but also outside to make average annual estimates of soil loss due to wind erosion. But, because both are empirical models, their application outside the USA is somewhat limited.
Nowadays the Agricultural Research Service (ARS) is developing a new Wind Erosion Prediction System (WEPS) to overcome the limitations of the WEQ. WEPS will make daily estimates of soil loss due to wind erosion and account for variability that occur across a field in time and space. This system will be computer-based and make extensive use of existing natural resource databases. Major subroutines of this system will account for the effects of weather, soils, hydrology, tillage, crops, decomposition and the erosion process.

1.2 Soil properties

The properties to describe soils can be placed in one of the two classes:

1) properties that are more or less static and change very slowly through time (intrinsic properties), or
2) dynamic temporal properties that change very rapidly in response to management or climatic influences

It is the status of temporal soil properties (such as surface bulk density or aggregate size distribution) that control daily soil wind erodibility. However, the intrinsic soil properties (clay, organic matter content) greatly influence the temporal soil properties response to climate and management.

Temporal soil properties of WEPS

The SOIL sub-model of WEPS needs information about micro-relief, aggregate properties, crust properties and loose erodible material. Only aggregate properties and loose erodible material will be discussed here, as these two properties are important for this study.

The aggregate properties can be subdivided in (Zobeck 1991):

- *Dry aggregate size distribution*

  Dry aggregate size distribution refers to the relative amounts of aggregates, on a mass basis by size class, present on the soil surface. The dry aggregate size distribution is determined by sieving dry surface soil samples using a rotary sieve. Knowledge of dry aggregate size distribution is needed for wind erosion prediction because the amount of wind erosion varies with the amount of erodible size aggregates present on soil surface.

  Although mineral soil aggregates as large as 2 mm can be moved by wind, aggregates greater than 0.84 mm are generally considered non-erodible by wind.

  Aggregates composed of organic or volcanic soil material generally have a larger critical aggregate size on account of their lower (bulk) density (Zobeck 1991).

- *Dry aggregate stability*

  Dry aggregate stability refers to the resistance of soil aggregates to breakdown from physical forces and is a measure of the strength of the binding agents within aggregates. The dry aggregates stability is important in wind erosion prediction because, in general, dry soils are struck by flying sand grains causing abrasion as part of the wind erosion process, and the amount of erodible sediment dislodged from aggregates is related to how well aggregates resist abrasion.

- *Dry aggregate density*

  Aggregate density, the ratio of the aggregate mass to the bulk volume of soil particles plus pore space in the aggregate, is of considerable importance in WEPS because it determines the velocity of wind needed to erode small soil particles and aggregates. It may be correlated with dry aggregate stability, and other temporal soil properties, as well as particle density of the individual grains.

Loose erodible material

Loose erodible material is defined as loose, unconsolidated soil material less than or equal to 0.84 mm. The amount and distribution of loose erodible material on the soil surface is related to the erosion potential of the soil. Loose erodible material lies on the surface, directly exposed to the forces of the wind. If loose erodible material is not present on the soil surface, erosion generally will not occur. As these materials are moved during an erosion event, they act as projectiles that cause further abrasion of the surface, producing more erosion.

Topography

In one of the earliest studies of the effect of knolls (hummocks, low dunes) on wind velocity and surface drag, the researchers found that over knolls with slopes up to about 1.5%, the lines of equal wind velocity (Figure 1) are virtually parallel and generally conform with a pattern that exist over level ground. But over knolls with slopes greater than 1.5 percent, the lines representing equal velocity are compressed, indicating that a steeper velocity gradient occurs there. The greater the slope, the steeper is the wind velocity gradient and the greater is the wind drag, only when the length of a slope does not exceed a certain limit. For a slope of 3%, the limit is around 100 meter, for a 10% slope it is about 250 meter. Beyond those limits the lines of equal wind velocity tends to follow the contour of the land.

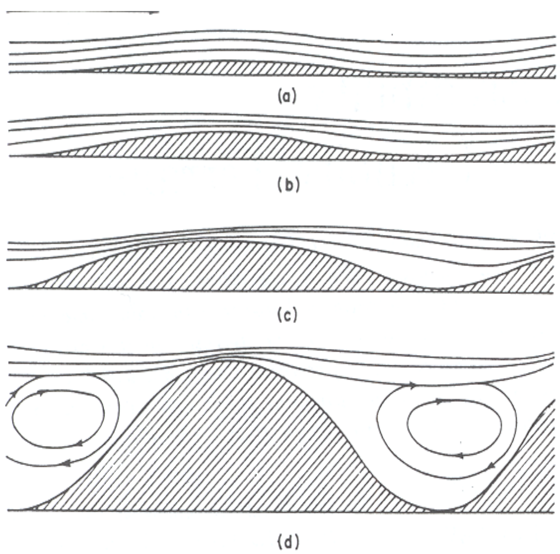

Figure 1. Lines of equal wind velocity

over
a) a change of elevation of 1.5%,
b) a knoll not exceeding 130 meter in diameter with 3 percent slopes,
c) a knoll not exceeding 130 meter in diameter with 6 percent slopes, and
d) ridges with slopes greater than 25%.
(After Doughty and Staff, 1943)
(Source: (Chepil, Siddoway et al. 1964)

Wind drag

As wind flows over the land surface, the surface exerts a drag such that an atmospheric boundary layer of approximately 1-meter is formed (Fryrear 2000). This boundary layer impacts the detachment (also called deflation), movement, and deposition of soil particles. When soils erode, the wind within this layer is defined as turbulent, This turbulent characteristics facilitates the transfer of momentum from the wind to the soil surface and exerts a drag or shear effect in the surface. This drag can be computed from the wind as follows.

$$\tau = \rho(U_*)^2$$

where

τ = wind drag, dynes m^{-2}
ρ = air density, gm m^{-3}
U_* = drag speed, m s^{-1}

Drag speed can be computed by

$$U_* = \frac{Uz}{5.75 \log(z/k)}$$

where

U_* = drag speed, m s^{-1}
Uz = wind speed at height z, m s^{-1}
z = height where Uz is measured, m
k = aerodynamic surface roughness, m

Drag speed can also be determined graphically using the relationship in Figure 2. The wind speed Uz is plotted as a function of the log of the height (z). From this plot the aerodynamic surface roughness (k) and drag speed (U_*) can be determined as the intercept and slope, respectively .

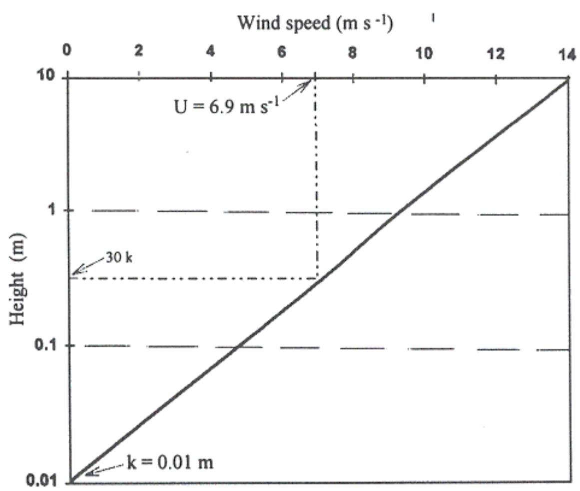

Figure 2. Determining aerodynamic roughness (k) and drag speed (U_*) graphically from plot of wind speed and height of wind speed measurement

According to measurements made by Chepil (1964), the angle of inclination of the drag speed is lower for knolly terrain. Therefore wind speed increases when measured on the same height above ground.

1.3 Global assessment of soil degradation with special reference to wind erosion

1.3.1 General

Since the 1970 the need of a global assessment of soil degradation was recognised world-wide. For planners it was impossible to know where soil degradation occurred because of lack of information. In Africa land degradation maps where non-existent at continental, national and local level (WASWC 1989). For planners these maps are needed to make correct decisions for land use.

Based on the recommendations of the UNEP meeting in Nairobi (May 1987) a project document was formulated entitled: Global Assessment of Soil Degradation, which would lead to the publication of a map at a scale of 1:10 million of human induced soil degradation (Oldeman, Lynden et al. 1997)

GLASOD included 12 soil degradation types in the world map.

Wt	Water erosion: loss of topsoil
Wd	Water erosion: terrain deformation
Et	Wind erosion: loss of topsoil
Ed	Wind erosion: terrain deformation
Eo	Wind erosion: Overblowing
Cn	Chemical deterioration: loss of nutrients and/or organic matter
Cp	Chemical deterioration: pollution
Cs	Chemical deterioration: salinization
Ca	Chemical deterioration: acidification
Pc	Physical deterioration: compacting, sealing and crusting
Pw	Physical deterioration: waterlogging
Ps	Physical deterioration: subsidence of organic soils

E: *Wind erosion*

Et: Loss of topsoil

This degradation type is defined as the uniform displacement of topsoil by wind action. It is a widespread phenomenon in arid and semi-arid climates, but it also occurs under more humid conditions. In general, coarse textured soils are more susceptible to wind erosion than fine-textured soils. Wind erosion is nearly always caused by a decrease of the vegetation cover of the soil, either due to overgrazing or to the removal of vegetation for domestic use or for agricultural purposes. In (semi-) arid climates natural wind erosion is often difficult to distinguish from human-induced wind erosion, but natural wind erosion is often aggravated by human activities.

Ed: Terrain deformation

Terrain deformation by wind erosion is much less widespread than loss of topsoil. It is defined as the uneven displacement of soil material by wind action and leads to deflation hollows and dunes. It can be considered as an extreme form of loss of topsoil, with which it usually occurs in combination.

Eo: Overblowing

Overblowing, which is defined as the coverage of the land surface by wind-carried particles, is an off-site effect of the wind erosion types mentioned above. Overblowing may occur in the same mapped unit as those other types, or in adjacent units. It may influence structures like roads, buildings and waterways, but it can also cause damage to agricultural land.

Furthermore two other mapping units were distinguished, areas which are not affected by human-induced soil degradation, stable terrain, and wastelands, including active dunes, deserts and salt flats.

1.3.2 Summary of the GLASOD methodology

Severity of soil degradation

The severity of soil degradation in GLASOD is an aggregation of the degree of soil degradation and the extent of the degradation process. This is illustrated in Table 1. The degree or intensity of soil degradation is related to observed changes in the agricultural suitability, productivity, and restoration potential and biotic functions at one particular location (Oldeman, Lynden et al. 1997). The extent of soil degradation is the relative frequency of occurrence of a particular type of degradation within the delineated map unit.

Table 1. Severity of soil degradation in GLASOD

Degree of soil degradation	*Frequency of soil degradation*				
	Infrequent	*Common*	*Frequent*	*Very frequent*	*Dominant*
Light	Slight	Slight	Medium	Medium	High
Moderate	Slight	Medium	High	High	Very high
Strong	Medium	High	High	Very high	Very high
Severe	Medium	High	Very high	Very high	Very high

Rate or trend of soil degradation

For planning purposes the recent past rate (for example last 5-10 years) of degradation is very important. A severely degraded area may be relatively stable at present, whereas some areas that are now slightly degraded may show a high rate. The latter area, in principle, has a higher conservation priority than the first one.

NB: Whereas the degree of degradation in fact only indicates the current, static situation, the rate indicates the dynamic situation of soil degradation, namely the change in degree over time.

1.4 Small-format aerial photograpy (SFAP)

1.4.1 General information of SFAP

Small-format aerial photography (SFAP) is becoming a popular alternative to commercial large-format aerial photography. SFAP can be defined as an image format with sides smaller than 12 cm (Chanond and Leekbhai 1986). The advantages of SFAP include the relatively low costs and flexibility of acquisition. The use of SFAP is recommended when:

1) Existing large-format aerial photographs are not available, and for
2) Use as supplement to large format aerial photographs (Meyer 1982).

SFAP offers a relatively lower cost alternative for short, specific, carefully timed large-scale photographic flights. It is far less expensive then metric small-format cameras and much easier to set up a standard small-format camera then a metric one.

Measurements from standard SFAP are less accurate than those obtained from metric aerial photographs. Factors such as a lack of lens calibration, absence of film flattening devices, lack of forward motion compensation, and the presence of lens distortion limits the metric qualities of SFAP (Faig 1976). Another factor that decreases the accuracy is the tip and tilt of the aircraft during the flight. This error can be partially compensated using GPS to georeference the SFAP. Before analysing, the SFAP is normally enlarged which decreases the accuracy of the SFAP. This enlarging process change image scale in an inconsistent manner, crops a portion of the image from the print and add additional distortion like tip and tilt in the photo (Needham and Smith 1984). Although the metric qualities of SFAP does not meet the accuracy standards of metric cameras, for cases like mapping soil and vegetation patterns the accuracy is acceptable.

1.4.2 Use of SFAP in mapping and measurements.

SFAP has been used for mapping and measurements. It is used to obtain information such as tree heights, crown width and crown area (Hagan and Smith 1986), and for computing ground coordinates and map waste sites. The resulting waste site map was not that accurate, but an error of three meters was acceptable (Warner 1994). Also SFAP is used to measure logging road system length. The results were adequate to determine forest road system area and the corresponding potential for erosion (Rowe, Warner et al. 1999). A digital camera is used to obtain digital images of 35-mm photographs where pixel counts were used to measure areas of wind erosion damage (Lyon, McCarthy et al. 1986). To measure changes in rangeland vegetation a helicopter-borne 35-mm aerial photography is used (Tueller, Lent et al. 1988). SFAP is most used for analysing urban housing problems, for example in Bangkok (Chanond and Leekbhai 1986).

1.4.3 Georeferencing SFAP

Most of the studies performed with SFAP do not mention any geometric correction. (Spencer 1998) describes the use of SFAP in the Australian forestry with special emphasise on monitoring of diseases. In this study monoplot was used to georeference the SFAP. As a complementary technology GPS was mentioned. Also Rowe (1999) mentioned the use of GPS in SFAP. But in most studies the use of GPS is only limited to navigating the aircraft. No study mentions the use of GPS to georeference the SFAP.

Global Positioning System (GPS)
With the aid of GPS, coordinates of object, which can be used as tiepoints for georeferencing, are easily to obtain. In short, the system consists of 24 satellites with known positions, which sends signals to receivers. A logarithm within the receivers calculates the position of this receiver with aid of the different signals received. Depending on the type of signals that can be received, and method to calculate the positions, precision ranges from centimetres to more than 10 to 15 meters.

1.5 Rectification

1.5.1 General information

In most aerial photographs the picture is distorted, with respect to the map geometry by

a) displacement of terrain features due to tilt of the camera photo plane, or
b) relief displacement due to height differences in the terrain: higher points are imaged further away from the nadir then lower points having equal distance to it in the terrain.

Both phenomena cause a distance- (and scale-) variation which does neither exist in reality nor in a topographic map. With proper techniques and in some cases knowledge of the terrain heights, the geometry of such images can be changed such, that the scale variation is practically removed. Thus the image will have the same geometry as the map.

1.5.2 Conventional rectification

Recommended for normal camera, i.e. small format photographs; conventional rectification; minimum of 4 tiepoints required;

Col = (aX + bY + c) / (gX +hY + 1)

Row = (dX + eY + f) / (gX + hY +1)

1.5.3 Differential rectification

Orthophoto georeference

The orthophoto georeference is recommended for photogrammetric camera aerial photographs when a DTM is also available. Like direct linear it also corrects for tilt and relief displacement. At least two fiducial marks, the principal distance, and a set of tiepoints in RowCol and XYZ coordinates have to be given. Height values are supplied by the user, or obtained from the DTM. The principal point (inner orientation) is calculated from the fiducial marks and the principal distance. Camera position (Xo, Yo, Zo) and angles (κ, ϕ, ω) are calculated from the tiepoints (outer orientation). Minimum of 3 tiepoints is required.

Direct linear transformation

Recommended for normal camera, i.e. small format photographs when a DTM is available. It will correct for tilt and relief displacement. Direct linear transformation (DLT) stores a set of tiepoints in RowCol and XYZ coordinates. Height values are supplied by the user, or obtained from the DTM. Outer orientation parameters, i.e. camera position (Xo, Yo, Zo) and camera axis angles (α, β, γ) are calculated from the tiepoints. Minimum of 6 tiepoints are required to solve the 11 parameters. The tiepoints must not be co-planar, i.e. the tiepoints should not be on a tilted plane.

Row = (aX + bY + cZ + d) / (eX + fY + gZ + 1)

Col = (hX + iY + j Z + k) / (eX + fY + gZ + 1)

Coplanarity

In a georeference direct linear, there is no inner orientation calculates. The principal point remains unknown. The location and tilt of the camera are calculated from the tiepoints only. When all tiepoints fit in one (tilted) plane in XYZ- direction, a projection centre can not be calculated. The tiepoints are coplanar and the matrix remains singular. At least two tiepoints must be outside the common plane. Special attention have to be made when the tiepoints almost fit in one (tilted) plane, the transformation does work but is not reliable (Hendriks 1999)

A georeference direct linear has the highest accuracy within the 3D envelop bounded by the tiepoints. The better the XYZ spread of tiepoints, the better the transformation will work. To obtain a reliable georeference, it is necessary that (at least) two tiepoints clearly deviate in Z-direction from a (tilted) plane.

1 The study area

1.1 Location and extent

The study area is situated in the Lake Naivasha catchment area in the central part of the Eastern Rift Valley. The Naivasha catchment is confined by the Nyandarua Mountains to the east (with elevations to over 3,960 m), the Mau Escarpment to the west (exceeding 3,000 m), to the south by Mt. Longonot (exceeding 2,400 m) and to the north by the Menengai Crater (exceeding 2,100 m). The study area itself lies at an altitude of approximately 2,100 m.a.s.l. The study area comprises about 360 ha, and is located between latitude 0^o 49' S to 0^o 53'S and longitude 36^o 27' E to 36^o 29'E, about 70 km Northwest of Nairobi (see Figure 1). Administratively, the area falls under the Naivasha Division of Nakuru District.

During fieldwork, pictures were taken to obtain a general view of land degradation in the reconnaissance area (see Figure 2). A pilot area was selected where the actual fieldwork has been carried out.

Figure 1. Location map of Lake Naivasha area (Source: www.maps.com)

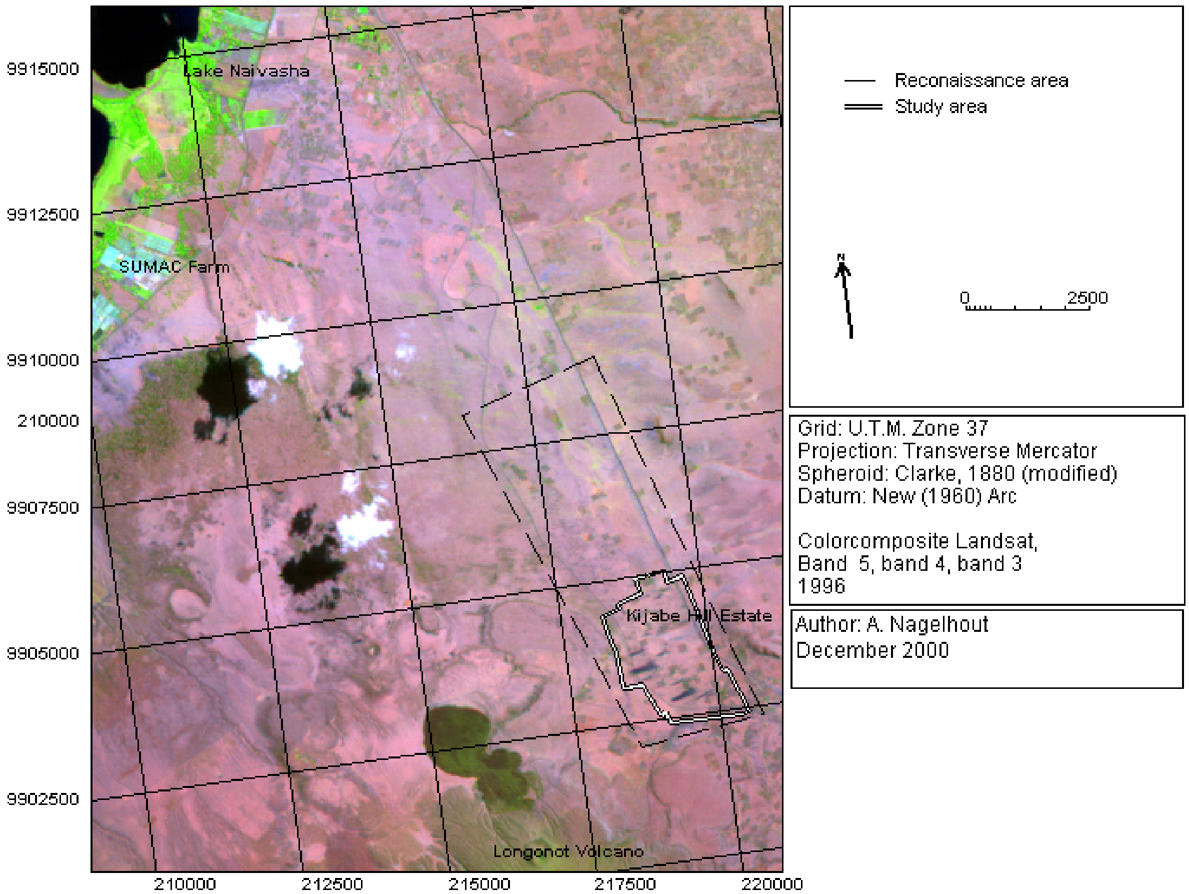

Figure 2. Location map of the study area Longonot-Kijabe Hill

1.2 Climate

1.2.1 Rainfall, temperatur and eva-transpiration

According to the Köppen's classification, the climate in the area can best described by a warm, temperature, rainy climate, with a dry season in the summer (Cs) (Elsevier 1989). The coldest month in the area has temperatures above 0°C, but below 18°C, and the warmest month is above 10°C.

Rainfall

The rainfall in the area is influenced by the Equatorial Monsoon climate hence there are two rainy periods. The main rainy season is from March to May and the short rainy season from October to December. The average annual rainfall of the area is about 608 mm/year for the period 1931-1960 (Ase 1986). This rainfall varies between 443-939 mm/year. For the period 1985-1995 mean rainfall at Naivasha was 760 mm/year. The lake area is a relatively low rainfall area compared to the neighbouring rift escarpments where rainfall is higher, ranging between 1250-1500 mm/year (Clarke 1979).

Table 1. General climatic data from Meteorological Station at Naivasha Airport, altitude: 1900 m.a.s.l. Coordinates 0°25' 48'' S 36°15'36'' E

Month	*Min. temp. (°C)*	*Max. temp. (°C)*	*Average temp. (°C)*	*Average rainfall (mm)**	*Humidity (%)*	*Sun hours*	*Radiation MJ/m2/ day*	*ETo mm/day ** *
Jan	8.0	27.6	17.8	34.5	62	5.3	17.1	3.8
Feb	8.1	28.2	18.2	40.2	61	5.9	18.5	4.1
Mar	9.7	27.2	18.5	54.0	65	5.3	17.8	3.9
Apr	11.5	25.0	18.3	136.6	75	4.7	16.3	3.4
May	11.2	23.7	17.5	88.3	80	4.9	15.8	3.1
Jun	9.8	23.0	16.4	37.5	79	4.8	15.0	3.0
Jul	9.2	22.5	15.9	26.2	77	4.2	14.4	2.9
Aug	9.3	22.8	16.1	42.2	76	4.7	15.9	3.2
Sept	8.7	24.5	16.6	46.7	74	5.4	17.7	3.6
Oct	9.0	25.5	17.3	49.8	72	5.5	17.9	3.8
Nov	9.2	24.6	16.9	53.2	77	4.4	15.8	3.3
Dec	8.6	25.7	17.2	43.8	72	4.2	15.1	3.3
Average	9.4	25.0	17.3	54.4	73	4.9	16.4	3.5

** Rainfall data from Naivasha Longonot Farm over the period 1948-1980*
** Evapo-transpiration values have been derived following the FAO Penman-Monteith method
Source: FAO's Cropwat

Temperature

The maximum temperature ranges from 24.6 ^{0}C to 28.3 ^{0}C with the highest temperature in January and February. The monthly minimum temperature range from 8 ^{0}C to 11.5 ^{0}C. Average monthly temperatures range from 15.9 to 18.5 ^{0}C with coldest months in July and August. Figure 3 shows these monthly temperatures. As the area is at an altitude of 1,900 m.a.s.l., temperatures do have strong fluctuations during the day. The study area lies approximately 200 meters higher than the lake area and temperature is therefore cooler, about 1 °C.

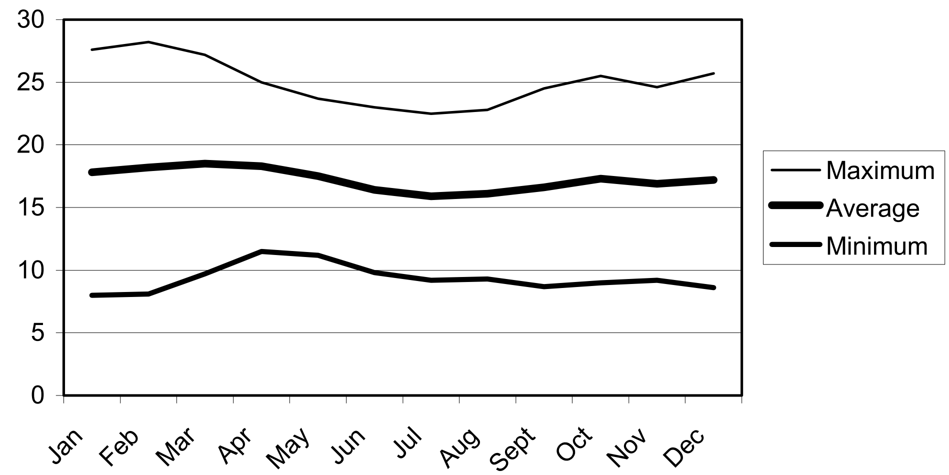

Figure 3. Monthly maximum, average and minimum temperature of the Naivasha area, (Source: Ministry of Land Reclamation, Regional and Water development)

Evapotranspiration

Relative humidity is low throughout the Rift Valley. It is 75% at Naivasha (Clarke, Woodhall et al. 1990), hence the potential evaporation of 1600-1800 mm exceeds rainfall. Mean monthly potential evaporation at Naivasha exceeds rainfall by a factor of 2-8 for every month, except April when potential evaporation still exceeds rainfall except in the wettest years (Clarke, Woodhall et al. 1990).

1.2.2 Wind regime

In the area, there is an increase of wind speed during the day. Because the area is situated on the floor of the rift valley, at the end of the day winds from the colder upper plateau enters the warmer valley with higher velocity. Table 2 gives values of wind velocity and direction. The data is from only one year from an area near the lake (Sulmac Farm). Observations are made with a 10 minutes interval. The wind regime in the study area will be different, but unfortunately no data is available from that area. The monthly average wind velocities are strongest in the months of May and June, but maximum wind velocities are reached in March and April during the rainy season, although in this particular year no rain has fallen in these months.

Table 2. Wind velocity and direction, October 1999-September 2000 (Sumac Farm)

Month	*Average (m/s)*	*Maximum (m/s)*	*Average wind direction*
Jan	3	25	Southeast
Feb	4	22	Southeast
Mar	5	27	Southeast
Apr	6	28	South
May	7	25	Southwest
Jun	7	23	Southwest
Jul	6	24	Southwest
Aug	6	24	South
Sep	6	23	South
Oct	5	26	South
Nov	4	20	South
Dec	4	19	South

On a yearly base almost 40% of the time, wind is coming from the south-west and only 3% of the time from the north-west (Figure 4).

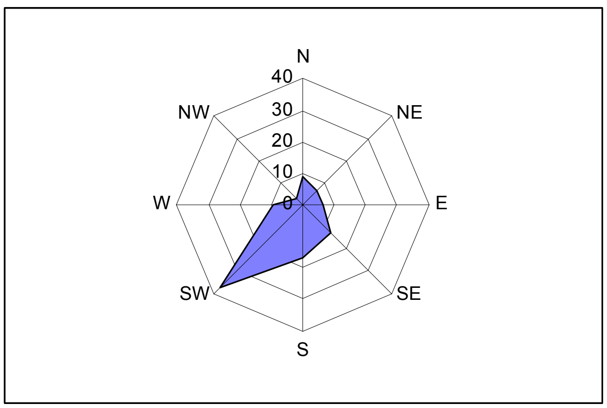

Figure 4. Prevailing wind direction on a yearly base

1.3 Geology

1.3.1 Regional stratigraphy

Geological information from the area is available in the form of 1: 50,000 geological map of Naivasha and geological reports of Naivasha (Clarke, Woodhall et al. 1990). The area around Lake Naivasha is geologically very young, with all rocks and structures having formed during the past 4 million years during 4 episodes of volcanic activity and faulting. Table 3 summarises the major volcanic and deformation episodes of the area.

The basin may be described as a graben, which is defined by major NNW-SSE trending faults. The floor is gently sloping and its highest point is around the study area, sloping northwards to 300 m.a.s.l and southwards to 600 m.a.s.l.

Table 3. Major volcanic and deformation episodes of the Naivasha area (adapted from Clarke et al, 1990)

Volcanic episode	*Activity*	*Units*	*Age range*
V4	Late Quaternary to recent Salic volcanoes	Longonot, Olkaria, Elementita, and Akira Volcanic groups, Fluvio and Lacustrine sediments	0.4 Ma
D4	Extensive minor faulting of rift floor		0.8-0.4 Ma
V3	Quaternary flood lava's of rift floor	Gilgil trachyte, Kijabe Hill formations	1.65-0.9 Ma
D3	Renewed faulting of rift margins		1.7 Ma
V2	Early Quaternary flood trachytes	Limuru Trachyte, Karati Basalt Formations	2.0-1.8 Ma
D2	Formation of step faults (narrowing of graben)		3-2 Ma
V1	Pliocene volcanic ash flows	Kinangop tuff and Mau tuff formations	3.7-3.4 Ma
D1	Major faulting of eastern rift margin		4-3 Ma
V = Volcanic activity, D = Faulting activity			

1.3.2 Geological units of the study area

The major units at the surface of the study area are (see Figure 6):

a) *Mixed Akira pumice (Lpa) and Longonot Ash (Lp8)*

This unit forms the larger part of the study area. It is formed around 3280 ±120 years BP from paleosol immediate below, bedded ash overlays thin basal pumice lapilli. It was formed from magmatic an phreatic-magmatic eruptions.

b) *Lower Longonot trachyte lava flows and pyroclastic cones (Lt2)*

This units exist of trachyte lava flows with blocky flow surfaces, and at least some with basal agglutinate (lithic rich).

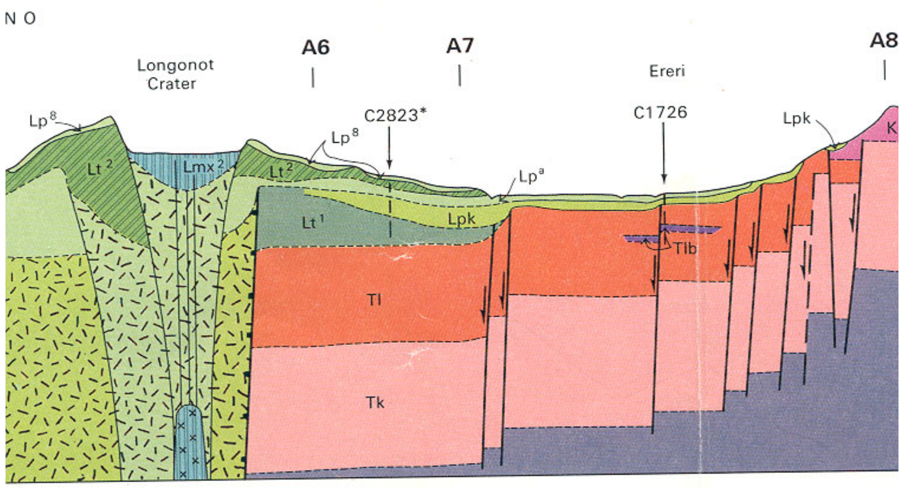

Figure 5. Geological cross-section of Longonot Volcano and Kijabe Hill

Below the surface (see Figure 5) the major units are:

c) *Kedong valley tuff, trachytic ignimbrites and associated fall deposits (Lpk)*
Major outcrops are found north-east and east of Longonot, inclusive flanks of Kijabe Hill and in some gullies of Longonot. At least 5 ignimbrite units each with weathered zone and paleosols (reddisch brown at top. The lowest ignimbrite is welded, the rest is partly welded.

d) *Limuru trachyte(Tl)*
This formation is formed around 1.66 – 2.65 million years BP. t is found on the eastern rift margin, especially on the old Naivasha road down Kikuyu escarpment. It consists of lava flows of trachyte and rhyolite composition. Some flows have abundant feldspar phenocrysts.

e) *Kinangop tuff, from the eastern rift margen (Tk)*
This unit is formed around 3.4-4.5 million years BP on the eastern rift margin. It consists of mostly welded tuffs, paleosols and weathered zones at top of most beds.

1.4 Geomorpholgy and soils

Landscapes

According the geopedological approach 4 landscapes can be distinguished in the Naivasha area.

- The Step-faulted Plateau
- The Volcanic Lava-flows Plateau
- The Volcanic Plain, and

- The Lacustrine Plain

Detailed information of the first three landscapes can be found in Chapter 5.

Figure 6. Geological map of the study area

The lacustrine plain occurs around the shore of Lake Naivasha and extends from about 1850-1920 m.a.s.l. The plain is largely covered with sediments of the surrounding volcanic rocks of the rift margins. Despite their extensive distribution, the lake sediments are not thick and rarely exceed 30 m (Thompson and Dodson 1958). At the level of relief and moulding, low, middle and higher terraces differentiate the plain. The terraces have been formed by fluctuations of the lake water level.

Soils
Various studies at different levels of intensity have been carried out on the soils in the area. The pattern of the soils in the Lake Naivasha Area is quite complex and influenced by intensive variation in relief, climate, volcanic activities and underlying rocks (Sombroek, Braun et al. 1982). The soils are mainly formed from weathered volcanic and basement rock systems. More information about the soils in the study area can be found in chapter 5.

1.5 Vegetation

The main natural vegetation in the survey area is grassland with dwarf *Acacia tortillis*, and *Acacia seyal*. Livestock and wildlife mainly graze this type of vegetation. A large part of the natural vegetation has been cut and replaced by agriculture and pasture. The remaining vegetation has been partly disturbed by clearing except for some areas, which are conserved as National Parks.

1.6 Land use and agriculture

The area was formerly a ranching zone under European settlement (Marula Rangeland Estate) and supported large herds of cattle, sheep and goats. Creation of the European settlements had moved the Maasai from this formerly high potential dry-season grazing land to other drier areas.

With the arrival of European settler considerable changes occurred in the land use. They introduced ranching, diary farming and irrigation. Later the introduction of horticulture crops and flower cultivation around the Lake made this area one of the most important economic areas of Kenya.
In the study area, in the late 1960s and early 1970s the 'landless' population from Central Province of Kenya, started forming land-buying companies, which later bought a large percentage of the area. These companies subdivided the farms into smaller units of 5-acre plots, which were allocated to their shareholders. During the sub-division, the lay-out of the farms disregarded the natural features such as slopes, crest lines and drainage lines.

In 1990s wheat farming was started in the southern part of the general study area. Initially, probably due to favourable conditions (good climate and fertile soils on more else a gently undulating plane) yielded a bumper harvest in the first 1 or 2 harvests. In farm preparation, extensive vegetation cutting and tillage by heavy farm machinery's was done with anticipation that it would become a viable commercial project. Tree and shrub removal and cultivation exposed the area to highly erosive winds. This was done against the earlier technical advice from the Kenya Soil Survey. Then from 1992 onwards there was a persistent drought in the area leading to major crop failure. This led to farm abandonment. Abandoned arable fields had little shelterbelts or fences (Ataya 2000).

1.7 Tourism and wildlife

The lake and its surrounds are fragile with dynamic ecosystems and divers habitats. Numerous game parks and game reserves are established in the area. It supports a large variety of animals like waterbucks, giraffes, hippos, impalas and zebras. Also bird life is prolific in the area, with flamingos, fish-eagles, ibises and other wildfowl.

1. Materials and methods

1.1. Materials used

The following materials were used for this study:

- Topographic maps at scale 1:50,000
- Geological map at scale 1:50,000
- Aerial photographs at scale 1:20,000 (Kenya Geomaps, Western Pipeline (number 290-292)
- GPS receiver (Garmin 12)
- Soil sampling and digging tools (augers, knife, bags)
- Equipment for soil description (Munsell Soil Chart, pH, HCl)
- Data processing software (ILWIS 2.23, ILWIS 3.0 Alpha 32)
- Presentation and documentation software (Office 97)

1.2. Pre-fieldwork

The pre-field work phase included a number of preparations. Based on the objectives, a method was laid out to obtain the final wind erosion and land use change 1991-2000 (Figure 1).

General information
Data and information of the study area (Lake Naivasha) was collected to become familiar with the area. A reconnaissance area was selected on basis of earlier studies.

Soils and landscape of the reconnaissance area
The preliminary geopedological map of the reconnaissance area was elaborated, based on a stereoscopic interpretation of the aerial photographs. The geopedological units were checked during fieldwork. The photographs were also used to obtain the land degradation map of the area of 1991.

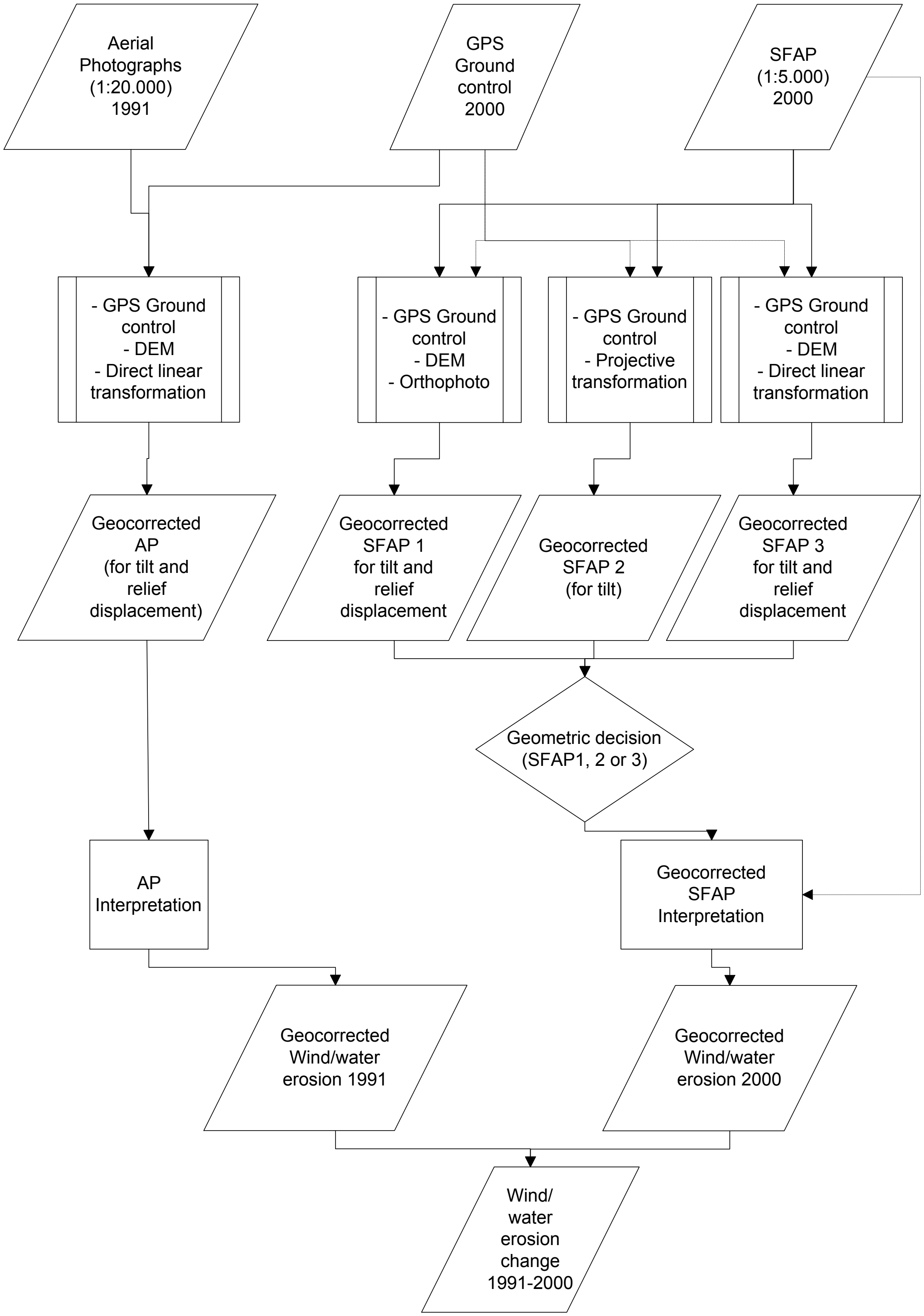

Figure 1. Procedure indicating successive steps to analyse land degradation changes (1991-2000), using SFAP as a complement to conventional aerial photographs

1.3. Fieldwork

During the fieldwork the following activities can be grouped into three major categories:

- Planning and generating of SFAP's
- GPS observation for rectifying SFAP's
- Analysing soils and landscape of the study area

1.3.1. Planning and generating of SFAP

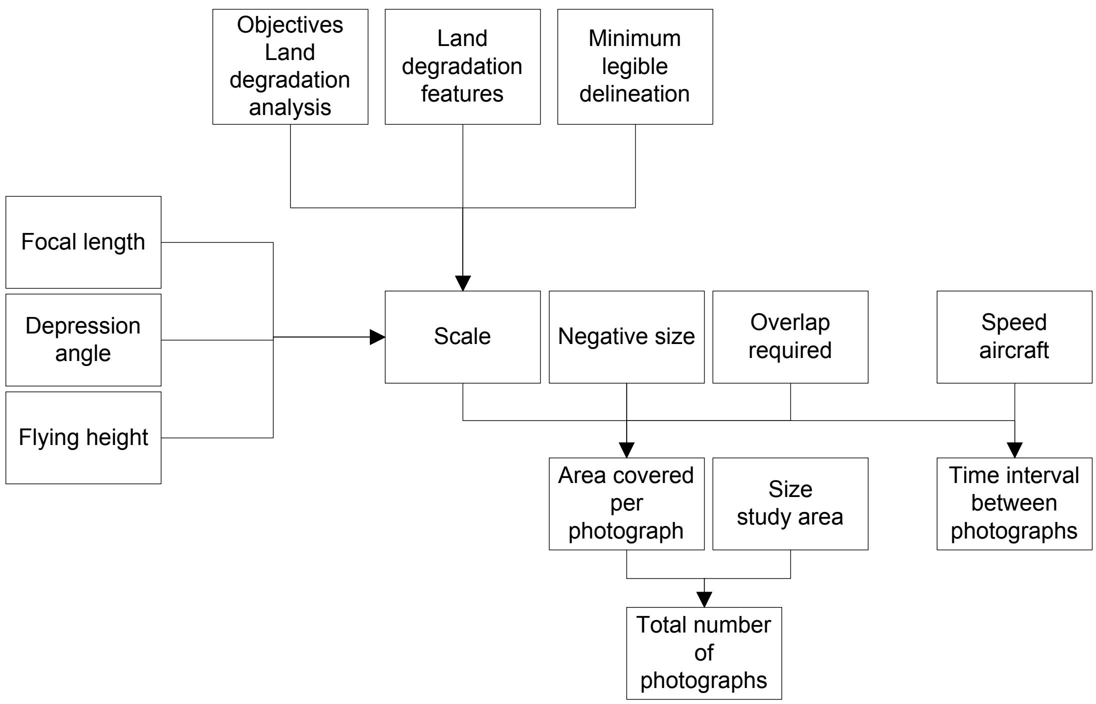

Figure 2. Small format aerial photographs flight planning

Figure 2 gives an overview of the factors needed to produce a flight plan for a study area, where the objectives of the study, the camera and size of the study area are important factors. The results of this process are the total number of photographs, with a certain scale to cover the study area.

Objectives land degradation analysis
The objectives are described in Chapter 1 under 1.3 Research objectives.

Land degradation features
The land degradation features to be distinguished on the photographs are especially wind erosion features like deflation trenches and deposition areas. If water erosion features can be distinguished, they also will be taken into account in this study. See also wind erosion features legend (**Error! Reference source not found.**).

System resolution
System resolution or photogrammetric resolution is an expression of the optical quality of an image produced by a particular camera system (Lillesand and Kiefer 1994). Some of the elements that have

influence on this resolution are the resolving power of the film (grain size), quality of the optical system and image motion

Minimum legible delineation

The minimum legible delineation is the smallest legible map area. This area is independent of map scale. It is conventionally defined to be a circular area of 0.4 cm2; the diameter of a circle with this area is 7.2 mm. Smaller delineation's are considered illegible for two reasons: 1) there is not enough room inside the delineation to write the map unit symbol, and 2) the proportion of the delineation becomes significant (Forbes, Rossiter et al. 1987). For the scales 1:5,000 and 1:10,000, the minimum legible area are 0.1 ha and 0.4 ha, respectively.

Focal length

One of the most important geometric features of an aerial camera is the focal length, which is the distance from the film plane to the centre of the lens when the camera is focused on infinity. Focal length is important for two reasons: it influences ground coverage and scale.

Depression angle

The depression angle is normally expressed as vertical, low oblique and high oblique. In this study the photographs are taken in the vertical position, perpendicular to the terrain, as this give the least scale differences in the photographs. When using low or high oblique, the photographs will have different scales throughout the photograph. Normally these scales are expressed in scale near, scale centre end scale far.

Flying height

The combination of the size of the features to be investigated, and the minimum legible delineation gives the desired scale of the final negative or photograph. In combination with the focal length, scale defines the flying height. The higher the flying height, the smaller the scale. For erosion feature mapping a scale of 1:5,000 for the photograph (10x15 cm) or 1:20,000 for the negative (24 x 36 mm) was selected.

Together with the size of the land degradation features to be mapped and the minimum legible delineation, the scale of the negative or photograph can be defined. Scale, negative size and required overlap gives the area covered per photograph. When the speed of the aircraft is included, the time interval between two photographs can be calculated.

Negative size

Small format aerial photographs are, by definition, all negatives smaller than 130 mm (Warner, Graham et al. 1996). The common ones are 36 x 24mm, 60 x 60mm and 70 x 70mm. In this study the negative size of 36 x 24mm is used as this is the standard for normal mirror reflex cameras. The advantage of this size is that it can be processed in all photo laboratories, mostly within the hour or day.

Overlap

For a stereoscopic view of the area, an overlap of minimal 50% is needed. A standard value of 60% is often used. The more overlap, the more photographs have to be taken of the same area.

Area

The area covered by one photograph depends on the negative size, scale and overlap. When these are determined, the size of the effective area (forward gain x sideways gain) is calculated. The size and form of the study area defines the length and total numbers of flightlines. Knowing the length of the flightlines, the number of flightlines and forward gain per photograph, the total number of photographs can be calculated.

The flight

During the flight a Minolta X300 camera with a 35-70 mm zoom lens was used. This restricted the options of some of the parameters that have to be considered for the flight planning. Table 1 gives the values of the different parameters.

As the final scale of the negative was set at 1:20,000, the focal length and flying height was defined at 35 mm and 2,300 feet (700 meters) above terrain respectively. The safe minimum speed of the aircraft (Cessna 182) with still good flying conditions is around 80 knots (148 km/hr). With a required overlap of 60 percent, the time interval between 2 photographs was calculated to be 7 seconds. The spreadsheet for this calculation can be found in Annex 2 (J.P. Horn)

Table 1. Parameters and values for small format aerial flight planning

Parameter	*Value*
Focal length	35
Negative width (mm) (along track)	36
Negative height (mm) (across track)	24
Depression angle (degrees)	90
Flying height (feet)	2,300
Terrain elevation (feet)	6,950
Flight Altitude (feet)	9,255
Scale centre	20,000
Depth coverage (m) (across track)	480
Ground speed knots	80
Ground speed (m/s)	41
Overlap required (along centre) (%)	60
Overlap required (lateral) (%)	30
Forward Gain (along centre) (m)	288
Lateral Gain (m)	341
Time interval (seconds)	6.99
Exposure time	1/500

Using the colour-composite of the LANDSAT image 2000, the position of the flightlines was entered on the image and coordinates were calculated. Every flight line had a 3 kilometre entrance line to guide the pilot to the first point of the study area. Coordinates of the first point of the entrance lines, first points of the study area and the last point of the study area were calculated. These coordinates were entered manually in the GPS (GARMIN III plus) of the aircraft, owned by a very experienced pilot Mr. Angus Simpson.

On Saturday 23rd of September 2000, after two weeks of sub-optimal weather conditions, the flight took place in the morning. The weather conditions were good, with some clouds around the study area, but without shades within the area. The door of the aircraft was taken out and the camera was mounted on a tripod in such a way that the lens would be just outside the aircraft. The tripod itself was tightened to the floor and the chair of the aircraft. The horizontal position of the camera was manually (with the eye) levelled. A second person was reading the display of the GPS from the moment the aircraft entered the flightlines. His task was to mention the moment when the actual taking of photographs had to start and to observe the overall performance of the flight. The third person, the author, made the photographs and changed the film after each flightline.

The aircraft took off at 9.00 a.m. and at 9.15 a.m. arrived at point 1 to enter the first flight line. 35 minutes later the 5 flightlines were flown and around 130 photographs were taken. During the flight the conditions were good with only one lateral gust of wind, at the beginning of the second flight line B (see **Error! Reference source not found.**).

Analysing the 130 photographs for land degradation features, the final study area was selected. Partly because in most parts there was no evidence of severe land degradation and because of time constraint, it was not possible to make GPS and land degradation features observation of the whole area. 28 Photographs were selected of which 14 were used to annotate the GPS observations and land degradation features.

1.3.2. Rectification of SFAP's

To rectify the SFAP's, GPS observation were made. The first idea was to use a differential GPS system (GARMIN Survey 100) to obtain coordinates with a precision of just a few meters. In the field problems arose with this system as data could not be downloaded and also high cost of batteries. Instead of this system a GARMIN 12 navigator was used.

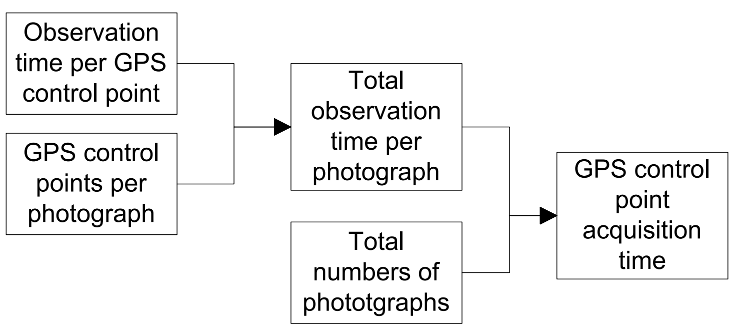

Figure 3. GPS observation planning

GPS control points per photograph

The number of GPS observation required per photograph depends on which method will be used to do the rectification, and this depends on the height differences in each photograph. Furthermore every rectification method needs a minimum number of control points (see paragraph 2.4).

Table 2. Minimum number of control points needed for transformation method

Transformation method	*Unknown parameters*	*Minimum control points*
Direct linear	11	6
Projective	8	4
Orthophoto	6	3

Another important consideration is whether the control points are only to be used for connecting the photographs, or also to improve the general geometry of the photograph. In that case more GPS observations have to be made. The advantage of making much more observations is that in case of a high error, found during rectification, points can be disabled to improve this error.

Observation time per GPS control point
Before May 2000, the Defence Agency of the United States who is the owner of the GPS-system, used the Selective Ability to reduce the accuracy of the GPS signals. But as the use of GPS has increased the last years in al kind of civil activities, the decision was taken to disable the Selective Availability. This means that the observation time at a point with a GARMIN 12 has reduced significantly to obtain the same accuracy.

Points for measurement were chosen in order to be clearly visible on the images. These normally consists of corners of farms, but also bushes, sharp corners of deflation trenches, electricity poles, constructional works etc, At every point a 5 minute observation was made in which the GPS calculated the average of 30 observations (epochs of 10 seconds). In total around 180 point were measured in a 3 days time period.

As the total amount of photographs and the total observation per photograph is known, the GPS control points acquisition time can be calculated. Transport time between and overlap of GPS control points are to be taken into account.

1.3.3. Soils and landscape of the study area

During fieldwork the geopedological units were checked and delineations were corrected. Soil descriptions and an inventory of degradation features were made to obtain specific information of the area. A wind erosion feature legend was constructed and codes were annotated on the photographs with additional information like depth and colours.

1.4. Post fieldwork

Rectification of SFAP
For the rectification of SFAP’s two activities were carried out. First a quality control of the GPS observations were made to obtain information about the precision. Secondly, the SFAP’s were rectified using three different methods, direct linear transformation, projective transformation and orthophoto rectification. An analysis of the results was made and the best method for that area was selected.

Soils and landscape of the study area

Using the observations from the field, the geopedological map has been reinterpreted and digitised using ILWIS to obtain the final geopedological map of the area. Soil samples were selected to be analysed, routine techniques to determine pH, texture, etc, and analysis to differentiate vitric or non-vitric properties. Due to logistical circumstances, the results of these analyses were not available to be included in this study.

Analysis of current wind erosion status

The new SFAP's of 2000 have been interpreted to obtain the current wind erosion status, using the wind erosion feature legend (see **Error! Reference source not found.**). The degree and extent of degradation were defined to obtain a severity classification of the land degradation features in the study area.

Spatio-temporal analysis of wind erosion

Loss of area during the period 1991 –2000 is calculated, using the land degradation status of these two years. Volume losses are also estimated during that period. Rates or trends of area and volume loss are established. Underlying factors as soil properties, existence of low dunes, land use and infrastructure are analysed to explain the rapid expansion of wind erosion in the study area.

1. Results and discussion

1.1. Generation of Small Format Aerial Photographs

1.1.1. GPS quality testing

To test the quality of the GARMIN 12 GPS, a set of observations have been made at an established benchmark ITC-1, behind the ITC building. The coordinates of this benchmark are given in the datum "Rijksdriehoekmeting" (Sharif 2000) and have been transformed to WGS84 using ILWIS 2.23. In total, 20 observations of 5 minutes each (averaging mode) were made during 2 months at different times, and information is presented in Table 1 and Figure 1. The distance between the coordinates of GPS observation and the actual coordinates are calculated. During the observations an indicator EPE (expected position error) gives a value about the actual horizontal precision in meters, an indication of the quality of the position. Although this EPE is not stored, values were slightly higher during observations at ITC then during fieldwork. A correlation between EPE value and distance does not exist.

Table 1. Statistical information of 20 GPS observations with GARMIN 12 at ITC-1

Function	*dX (m)*	*dY(m)*	*Distance(m)*
Minimum (point)	-1	0	1
Maximum (point)	-4	-11	11.7
Mean	0	-3	4.5
Standard deviation	2.3	3	2.7

The results are surprisingly good with 85% of the observations lying within 6 meters from the benchmark. The other observations (15%) have a range between 9.0 and 11.7 meters. Before May 2000, when the Selective Availability was still turned on, results like these could not have been obtained, consequently the use of GARMIN 12 GPS for this kind of work would have been impossible.

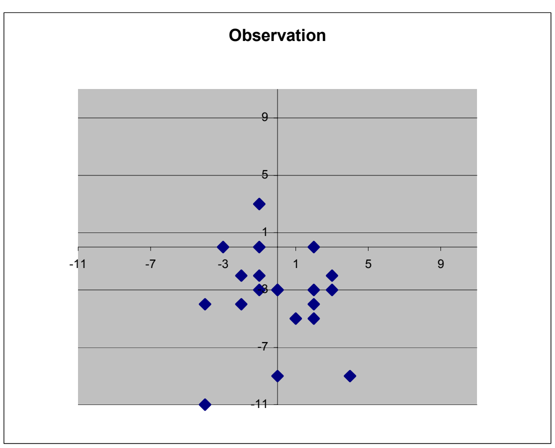

Figure 1. Scatter diagram of GARMIN 12 observations at benchmark ITC-1

1.1.2. Resulting flightlines

Flightline pattern

Figure 2 presents the flightline pattern covering the area. In total 5 flightlines were calculated using the spreadsheet and the parameters described in chapter 4.3.1 and 4.3.2. The distance between two flightlines is around 340 meters.

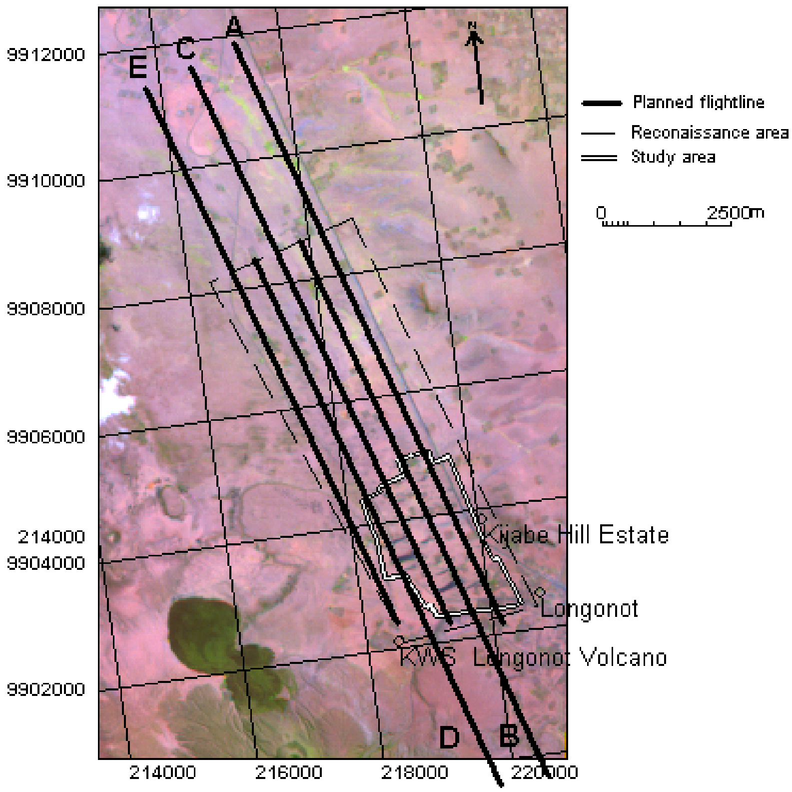

Figure 2. Planned flightlines covering the reconnaissance area

For the study area the position of the alternate SFAP photographs relative to the planned flightlines is presented in Figure 3.

The actual flightline A is flown in a straight way, whereas flightline B shows a sharp curve between the first and second photograph. This is because at that moment the aircraft was thrown aside by a lateral gust of wind causing a lateral displacement of the aircraft. The first photograph of flightline B is missing due to an error. Flightlines C en D are again more straight.

Four factors have influenced the quality of the flight: wind velocity, low speed and low weight of the aircraft and the experience (routine) of the pilot with specific kind of flight operations. Also in the area very strong winds do occur and for a not experienced survey-pilot, it will be very difficult to fly straight with a low speed.

Forward overlap between SFAP photographs is generally between 50% to 75% as alternate photographs do overlay each other. Lateral overlap in general is also sufficient, on average 20%. Only where the aircraft was hit by a lateral gust of wind (between B1 and B2) the overlap is 0%, for the remaining photographs it is up to 70%. The study area is 97% covered by SFAP's. Two small areas are not covered because of the problems as indicated above.

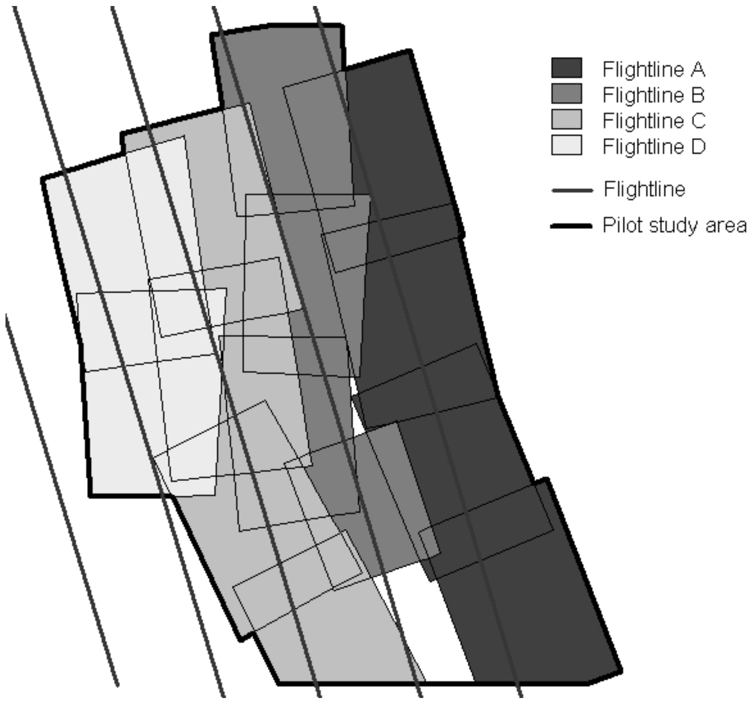

Figure 3. Actual position and overlap of SFAP's (projective transformation) and planned flightlines

Camera position

Table 2 presents an overview of the position of the camera at the moment of exposure. These values are obtained from the additional information of the direct linear georeferencing option of ILWIS. Flightline B has a very good overall performance with inclinations between 0.1° and 3.0°. Flightline C has a more varied performance with values between 0.5° and 14.9°.

Although flightline B suffered from lateral gusts of wind affecting the position of the aircraft in respect to the planned flightline, it did not affect the inclination of the camera. True vertical photographs have inclinations of less than 3°; in this case 9 photographs fall under this definition, the others could be classified as low oblique photographs.

Table 2. Inclination of the camera during exposure for the different SFAP's (direct linear transformation)

SFAP number	*Camera position (in degrees)*			
	X-axis (tilt)	*Y-axis (tip)*	*Z-axis (skew)*	*Inclination*
A18	87.8	90.0	177.8	3.1
A20	87.7	89.8	177.8	3.2
A22	93.7	89.8	3.7	5.2
A24	86.9	88.4	176.5	5.0
B00	89.9	90.0	0.1	0.1
B01	89.9	89.9	179.9	0.2
B03	91.4	89.9	1.4	1.9
B05	88.4	88.6	177.9	3.0
C18	81.9	96.8	10.5	14.9
C20	88.9	91.0	178.5	2.1
C22	90.1	92.2	2.2	3.1
C24	89.8	90.3	179.7	0.5
D05	90.4	87.5	2.6	3.6
D07	85.9	85.5	173.9	8.6

1.1.3. Scale and visual quality of SFAP

Scale

In Chapter 4.3.1 the required scale was set at 1:5,000of the final product (the photograph), the scale of the negative is 1:20,000. This would give images of sufficient resolution to study the wind erosion features in the study area. The scale of the photographs varies between 1:4,800 and 1:5,300, whereas the photographs within the same flightline have even less variation in scale.

Visual quality

The visual quality of the SFAP's is good to excellent. Objects like farmhouses, railway lines and roads are quite easy to distinguish (Figures 4). Even single trees and bushes can be distinguished as well as burrowing holes. Degradation features including wind erosion trenches, blown sand areas and vegetation changes can all easily be observed because of distinct colour contrasts with the surrounding non-degraded area. This is a major advantage over black and white photographs, where the contrast between degradation features and the rest of the image is generally much less. With the aid of a mirror stereoscope, the depth of deflation trenches and even small gullies can be assessed. Low dunes and even very low dunes can be delineated, but generally not in a consistent way as a general synoptical view of the larger dune complexes is missing and it is difficult to delineate such units as several SFAP photographs cover them.

Figures 4. Examples of a non-corrected Small Format Aerial Photograph

An important feature that could not be detected on the photographs was the re-growth of grass around deflation trenches and deposition areas. When sand is blown out of deflation trenches to grassland around these areas, the moisture is preserved in the surface soil due to the mulching effect of the ash deposits. From the ground with a low horizontal viewpoint of the observer these areas look quite green in comparison to the surrounding area. From the air with a high vertical viewpoint of the observer these areas can not be distinguished because of the a) predominant grey colour of the sand deposits and b) the vertical angle of the grass re-growth.

1.2. Rectification of SFAP

1.2.1. Application of direct linear transformation

In this Chapter the three transformations methods will be analysed and their overall performance will be assessed. For rectification the negatives were scanned on a resolution of 450dpi.

Referring to Chapter 2, direct linear transformation is recommended for small format aerial photographs without fiducial marks and only when a digital elevation model is available. The photographs of the study area have been georeferenced with at least 11 tiepoints (see
Table 3). The average pixel size is 0.47 m and the average error is 1.19 m. Only one photograph (C18) appeared to be coplanar, when all GPS observations are used. Reducing the number of tiepoints can improve the sigma and the geometric quality of the photograph.

Table 3. Sigma values before and after correction, pixel size and calculated error per SFAP photo (direct linear transformation)

SFAP number	*GPS points measured*	*Sigma with all GPS points*	*Active control points*	*Sigma after correction*	*Pixel size (m)*	*Error (m)*
A18	16	4.73	13	2.65	0.47	1.25
A20	20	3.49	16	2.50	0.48	1.20
A22	22	5.95	15	3.29	0.48	1.59
A24	2	3.88	15	2.63	0.49	1.28
B00	14	6.80	11	2.95	0.41	1.21
B01	20	7.95	13	3.25	0.44	1.43
B03	15	3.92	12	2.28	0.43	0.98
B05	17	4.88	12	3.12	0.44	1.38
C18	19	Singular matrix	14	2.32	0.50	1.16
C20	20	6.77	13	2.63	0.49	1.30
C22	24	5.93	16	2.50	0.48	1.19
C24	15	4.81	11	2.74	0.46	1.27
D05	19	5.30	14	2.69	0.50	1.34
D07	15	3.86	12	2.63	0.49	1.30
Mean	18.3		13.4	2.73	0.47	1.28

Table 4 presents information about the outliner from the trendplane and estimated flying height during exposure. Analysing this table, two important observations can be made:

- Outliners do not deviate much from the plane, and
- Estimated flying height gives unlikely results.

This transformation works only reliable when tiepoints are not (almost) coplanar. Height differences of less than 3.5 meters imply that the plane is flat (or coplanar). Furthermore, the estimation of the flying height gives unlikely results. Only one photograph (A18) is taken from the correct flying height of around 700 meters above terrain. Others are even made below terrain level. This indicates that direct linear transformation is not the most reliable transformation for this study area.

Table 4. Height differences and estimation of flying height (direct linear transformation)

SFAP number	*Active control points*	*Outliner 1 from trendplane*	*Outliner 2 from trendplane*	*Estimated flying height (m) (distance to nadir)*
A18	13	0.63	0.65	784
A20	16	3.23	2.12	195
A22	15	3.60	2.01	-2,797
A24	15	1.40	1.25	530
B00	11	0.79	0.63	-117
B01	13	1.73	1.10	59
B03	12	3.53	1.63	-113
B05	12	0.98	0.68	84
C18	14	2.44	1.93	-1,107
C20	13	1.18	1.01	87
C22	16	1.19	1.11	-353
C24	11	1.19	0.78	106
D05	14	1.92	1.46	-157
D07	12	3.27	2.34	482

1.2.2. Application of projective transformation

When the direct linear does not give acceptable results because the terrain is too level, the projective transformation is the alternative which may give good results. Looking at Table 5, average pixel size and error are almost the same as with direct linear transformation. Unfortunately, the additional information of this transformation is very limited, estimations of flying height and outliners are not available.

Table 5. Sigma values before and after correction, pixel size and calculated error per SFAP photo (projective transformation)

SFAP number	*GPS points measured*	*Sigma with all GPS points*	*Active control points*	*Sigma after correction*	*Pixel size (m)*	*Error (m)*
A18	16	4.36	12	2.50	0.47	1.17
A20	20	3.63	16	2.86	0.48	1.37
A22	22	6.01	16	2.89	0.48	1.39
A24	2	3.78	15	2.53	0.49	1.24
B00	14	7.58	9	2.36	0.41	0.97
B01	20	8.36	14	4.93	0.43	2.12
B03	15	5.18	10	2.45	0.43	1.05
B05	17	4.77	12	2.74	0.44	1.20
C18	19	4.80	14	3.26	0.50	1.63
C20	20	7.18	14	3.05	0.49	1.50
C22	24	5.79	17	2.78	0.48	1.34
C24	15	5.14	10	2.86	0.46	1.32
D05	19	5.42	14	3.04	0.50	1.52
D07	15	3.81	12	2.60	0.49	1.27
Mean	18	5.40	13	2.73	0.47	1.36

1.2.3. Application of Orthophoto transformation

Although the orthophoto transformation is not intended for use of photographs that are lacking fiducial marks, it is still possible to do so. The focal length, in this case 35 mm, and the flying height are known within a reasonable tolerance. The four corners of the negatives can be used as fiducial marks. As this transformation method is also designed for areas with higher internal relief, only three photographs are transformed in this way. The pixel size of the photographs is the same compared with the 2 transformations described before, but the sigma and calculated error is higher.

Table 6. Additional information of the orthophoto transformation per photograph

Photograph	*Active control points*	*Sigma*	*Pixel size (m)*	*Error (m)*
A18	14	2.92	0.47	1.37
A20	18	2.98	0.48	1.42
C18	16	4.04	0.50	2.03

1.2.4. Comparison and discussion of the results

The results of direct linear and projective transformation are compared:
1) pixel size, sigma and calculated error
2) analysing the overlap of edges of the small format aerial photographs, and
3) difference of actual GPS coordinates with their corresponding coordinates after resampling.

1) Pixel size, sigma and calculated error

The pixel sizes of the georeferenced photographs are exactly the same. Differences can be found in the sigma values of the photographs, although the average pixel size difference is only 0.2. Consequently the calculated errors also vary, but again the average calculated errors do not differ much, 1.29 against 1.36 for direct linear transformation and projective transformation respectively.

2) Overlap of edges

The edges of the resampled photographs (both methods) have been digitised and rasterised. The edges of the SFAP's georeferenced with the projective transformation are classified in distances of 1 meter, with a maximum of 20 meters. Both maps are crossed and distances between edges can be calculated. Figure 5 gives the results of this process. The total length of the edges is around 33 kilometre. Almost two-third of the edges lie within 2 metre of each other, and 95% of the edges lie within 9 metre of each other.

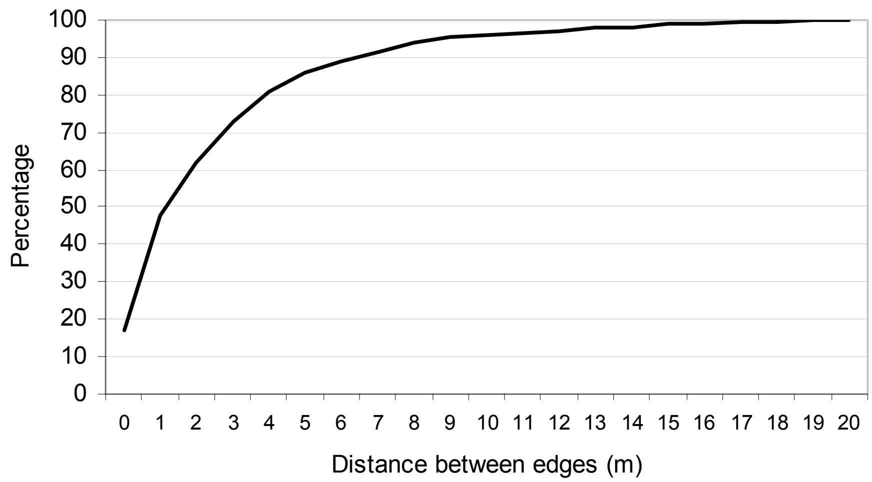

Figure 5. Classification of the distances between edges of SFAP's, georeferenced with direct linear transformation and projective transformation

3) Comparison of control points

Another way to compare the final result of the transformations is to compare the control points used to georeference the photographs (GPS observations) and their coordinates after resampling. Figure 6 shows a farm where three corners are measured with a GPS, the black squares. After resampling, of the same corners a point map is created (the white circles). The distance between these dots is calculated and classified in intervals of 1 meter (see Figure 7).

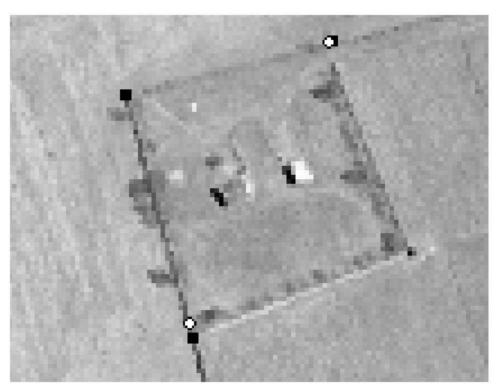

Figure 6. Comparison of GPS observations and control points after resampling

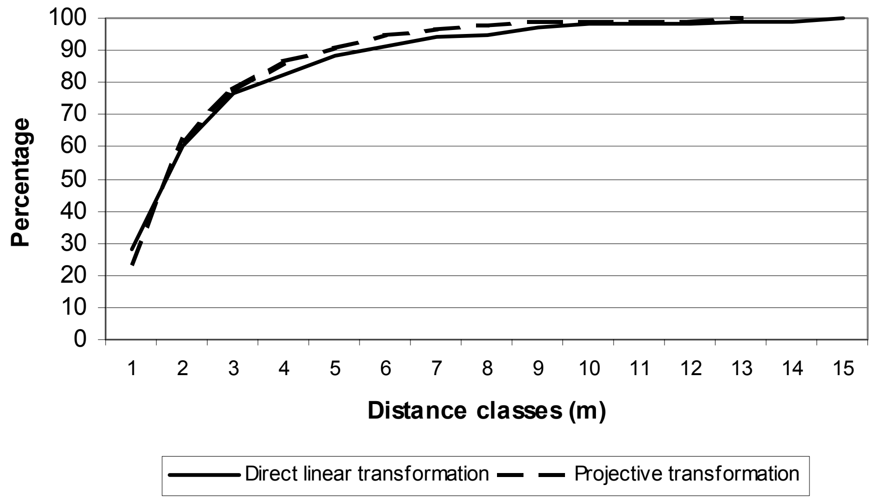

Figure 7. Distance classification of points measured with GPS in the field and corresponding position on the resampled photomosaic, using direct linear and projective transformation

Both transformations have almost the same results. For the projective transformation 95% of the points are within 6 meters, whereas for the direct linear transformation 95% is within 8 meters. These results do coincide with the quality testing of the GPS (Chapter 5.1.1.).

Some of the GPS observations have not been used as tiepoints for georeferencing. Al these observations (42 in total) have distance differences of more then 2 metre, 33% within 2 to 4 metres and 66% within 4 to 15 metres.

1.3. Soils and landscape of the study area

1.3.1. Geopedological analysis

After interpretation of the aerial photographs and field checking a geopedological map (see Figure 9) of the general study area was made, with the corresponding legend (see Table 7). In the study area three major landscapes were identified: The Step-faulted Plateau (Lf) to the east, the Volcanic Lava-Flow Plateau (Ll) to the west and the Volcanic Plain (Pv) in the central part.

Step-faulted Plateau (Lf)

The Step-faulted Plateau occurring in the eastern part of the study area forms the lowest part of a sequence of step-faulted plateau's of which the Kinangop plateau represents the highest level. It covers around 250 ha. Soils are moderately deep, around 90 cm, and relatively coarse textured and rock (stony) fragments in comparison with the Volcanic Plain. The lower horizons consist of depositions of lapilli and are strongly calcareous. These lapilli depositions are generally quite thick, up to at least 3 metres. Slopes vary between sloping (5-10%) and moderately steep (15-30%), with some dissected parts in the steep areas. On the mesa, around 100 meters above the Volcanic Plain the terrain is flat. Soils are deeper and there is more agricultural activity than in the Volcanic Plain.

Volcanic Lava-Flow Plateau (Ll)

The Volcanic Lava-flow Plateau in the western part of the study area covers the lower section of old lava flows from Mt. Longonot volcano. The extent of this unit is around 120 ha. The plateau lies only a 20-30 meter higher than the Volcanic Plain, divided by a very steep scarp, the front of a volcanic lava flow. Although no soil descriptions were made in this area, soils are probably not so deep or fertile, because there is almost no agricultural activity in this area.

Volcanic Plain (Pv)

The Volcanic Plain comprises the central part of the area and is the largest landscape, covering more than 460 ha. The study area is largely located within this unit, and therefore the focus of the remainder of this chapter will be on this landscape. The Volcanic Plain is very gently sloping (1-3%) from east to west.

Two relief forms are found, the plain itself and a vale. This last one is located at the foot of the scarp of the volcanic lava flows plateau. At landform level it is divided in 3 map units, all with the same slope between 1 to 3%. The distinction in 3 classes is made on the micro-relief, the presence of low dunes. These low dunes, or knolls, are an important factor in wind erosion as wind erodibility in areas with a pronounced micro-topography increases sharply (Chepil, Siddoway et al. 1964). The three classes are as follows:

- Volcanic Plain, very gently sloping (1-3%), without dunes
- Volcanic Plain, very gently sloping (1-3%), with very low dunes (0.3 to 2.0 m)
- Volcanic Plain, very gently sloping (1-3%), with low dunes (2.0 to 4.0 m)

1.3.2. Preliminary soil classification according to WRB 1998

General

The World Reference Base for Soil Resources (FAO 1998) has been used to classify the soils in the study area which are all developed on loose volcanic ash deposits from Mt. Longonot volcano. These deposits include Akira pumice (Lpa) and Longonot ash (Lp8). As analytical data is still missing at the time of writing, soil classification has been done on a preliminary basis.

Diagnostic horizons

The soils have no diagnostic surface horizon other than an *ochric* epipedon. The brown sandy Bw horizons never qualify as *cambic* horizon on account of their coarse texture. However, they are likely to meet the requirements of a *vitric* horizon in terms of (a) depth (< 25 cm from surface), and (b) mineralogical composition (> 10% of volcanic glass in the fine earth fraction), and (c) Al_{ox} + $½Fe_{ox}$ >0.4%.

Reference soil groups and subgroups

Having a *vitric* horizon within 100 cm from the soil surface and lacking an andic horizon overlying a vitric horizon the soils classify as *Vitric Andosols*. Further subdivisions can be made on the basis of

- their general sandiness (textures are loamy fine sand or coarser throughout the upper 50 cm of the soil) on account of which they qualify as *Arenic*, and
- their low base saturation (base saturation (by 1M NH4OAc) of less than 50 percent in at least some part between 20 and 100 cm from the soil surface) as a result of which the soils fall under *Dystric.*

The preliminary classification of all the soils observed is consequently *Areno-Vitric Andosol (Dystric).*

1.3.3. Establishing tentative soil phases

In this paragraph a tentative distinction of soil phases is described. This done in the absence of a) analytical data of the soils and b) a complete soil observation cover (even at semi-detailed level), as there was no time provision for this in this MSc-research.

According to the World Reference Base for Soil Resources (FAO, 1998), there is only one soil type in this study area as the diagnostic characteristics of the solums are practically the same. However, the soils show additional characteristics – often on the deeper subsoil – that are highly relevant to wind erosion analysis. For that reason 4 key soil properties were identified as follows:

- ❑ Presence and depth of Bw-horizon;
- ❑ Presence and depth of a loose dark grey sand layer;
- ❑ Presence and depth of a lapilli layer; and
- ❑ Presence and depth of a buried soil.

These properties form the diagnostic basis for the three soil phases.

Table 7. Geopedological legend of the study area (see also Figure 9)

Landscape	*Relief*	*Lithology*	*Landform*	*Map Unit*
Step-faulted Plateau (Lf)	Mesa	Limuru trachyte (Tl)	Summit	Lf111
		-do-	Shoulder complex	Lf112
	Escarpment	-do-	Steep, dissected	Lf211
		-do-	Steep, not dissected	Lf212
	Glacis	-do-	Upper part	Lf311
		-do-	Lower part	Lf312
	Alluvial fan	-do-		Lf411
Volcanic Lava- flow Plateau (Ll)	Mesa	Longonot ash (Lp8)		Ll111
	Scarp	Lower Longonot trachyte (Lt2); lava flows and pyroclastic cones.		Ll211
	Glacis	-do-		Ll311
	Hill	-do-	Low hill	Ll411
Volcanic Plain (Pv)	Plain	Akira Pumice (Lpa)	Very gently sloping (1-3%)	Pv111
		-do-	-do-, with very low dunes (0.3-2m)	Pv112
		-do-	-do-, with low dunes (2-4m)	Pv113
	Vale	-do-		Pv211

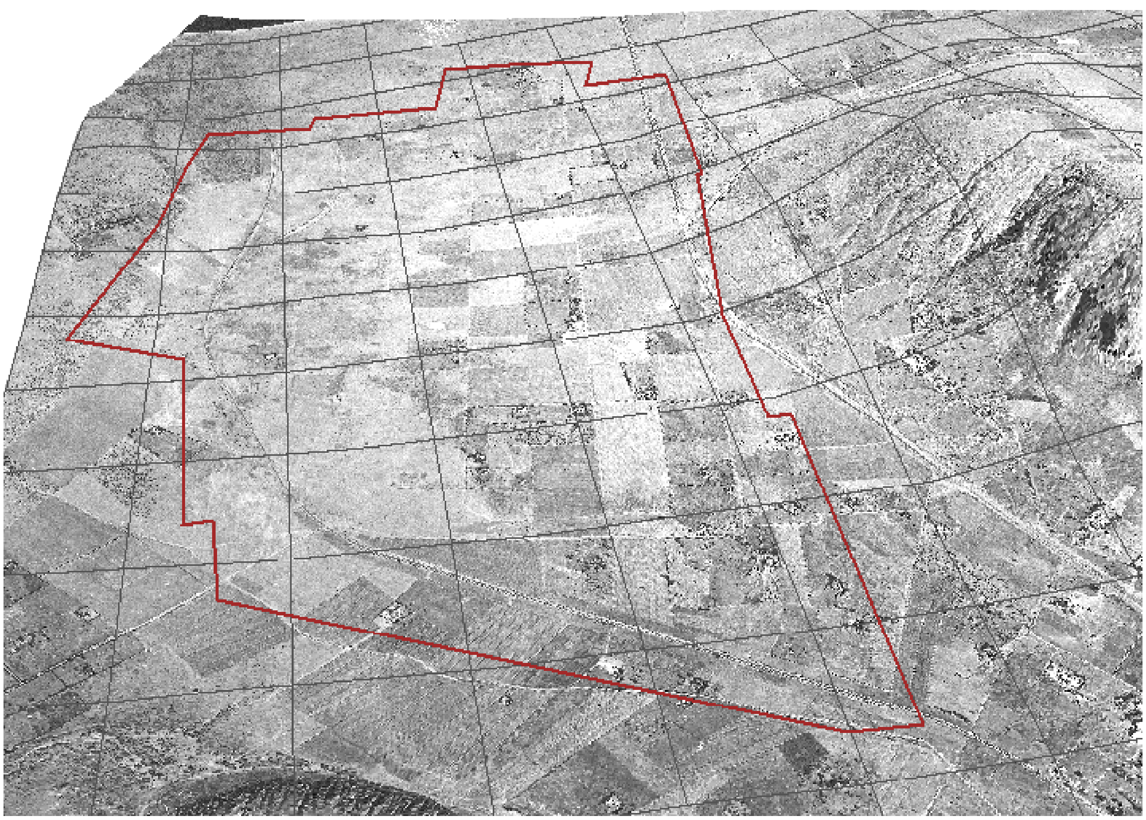

Figure 8. Three dimensional view of the study area

Figure 9. Geopedological map of the study area.

The thickness of the Bw-horizon varies between 24 to 72 cm. The thickness of only 24-cm in soil profile 008 is probably due to the planing effect of sand particles as this pit is in a deep sand deposition area. The lapilli layer consisting of Akira pumice gravel's, which is found in 4 pits within the profile description depth, is also found in soil profile 001 at around 3 m deep, and also seen at other locations like natural cuts, wells and by auguring. Normally, this layer occurs within 1 to more than 3 meters. The same applies for the buried soil (Bb) which is found beneath the lapilli layer and probably is also present in the whole study area. Looking at the thickness of the Bw-horizon and the presence of a dark grey sand layer a matrix can be made. The thickness is divided in 2 classes (more or less than 50cm) and absence or presence of a (thick) dark grey sand layer (see Table 8).

Table 8. Distinction of 3 major tentative soil phases on basis of a) thickness of Bw-horizon and b) presence/depth of dark grey C-horizons

		Thickness Bw horizon	
		20-50 cm	*> 50 cm*
Dark grey loose sand	Absent	A	-
	Within 50 cm depth	B	-
	Deeper than 50 cm depth	-	C

The reason for choosing these two parameters is to distinguish soils with a higher or lesser erodibility. Because the Bw-horizon in almost the entire area has the same texture (loamy sand) and a weak to moderate structure, it gives protection to the underlying layers when it is not disturbed. A thicker Bw-horizon will therefore give more protection than a thinner Bw-horizon. The wind erodibility of soils also depends on the presence of the dark grey loose sand layers in the subsoil which only occur in part of the study area. When the Bw-horizon disappears and dark grey loose sand appears at the surface, the wind erosion process will start.

Table 9. Specific information of 4 different properties of 9 soil profiles (Annex 1) and tentative soil phases

Map unit	*Pv1111*		*Pv112*				*Pv113*		*Lf312*
Soil observation (Naiv/2000/AN/xxx)	*002*	*007*	*004*	*006*	*008*	*009*	*001*	*003*	*005*
Thickness Bw	43	61	47	35	24*	54	79	72	40
Loose dark grey sand (upper boundary)	-	>91**	-	-	24***	81**	91	72	-
Lapilli layer (upper boundary)	69	Deep	76	55	Deep	Deep	Deep ****	Deep	92
Buried Soil (Bb)	108	-	104	95	-	-	-	-	>92**
Soil type	A	C	A	A	B	C	C	C	A

* Horizon Bw is under 42 cm of recent sand deposition
** Loose dark grey sand is not seen in the profile, but certainly present at deeper levels
*** Loose dark grey sand under Bw, but Bw is also covered with loose dark grey sand (see*)
**** Lapilli layer has not been observed in the profile but this layer occurs probably in the deeper subsoil throughout the study area (has been seen in natural cuts like wells, by auguring, etc).

Areno-Vitric Andosols (Dystric), soil phase A

A soil with a relative thin Bw-horizon (less than 50 cm) and absence of a dark grey sand layer. Within 1 meter a lapilli layer is found which covers a buried Bb-horizon. The erodibility of this soil is low. It is found in 3 map units, Lf312, Pv111 and Pv112.

Areno-Vitric Andosols (Dystric), soil phase B

A soil with a relative thin Bw-horizon (less than 50 cm) and presence of a C-horizon with loose dark grey sand within the first 50 cm. This soil is typical for depositional areas. The Bw-horizon probably got thinner because of abrasion by sand particles from the deflation trenches. It is found only in map unit Pv112.

Areno-Vitric Andosols (dystric), soil phase C

A soil with a relative thick Bw-horizon (more than 50 cm) and presence of a C-horizon with loose dark grey sand below the first 50 cm. This soil has a high erodibility risk when the Bw-horizon disappears. This soil is found in all three map units of the Volcanic Plain, Pv111, Pv112 and Pv113.

1.3.4. Description of major soils in the area

The soils on this area do have much in common. The A-horizon is absent in the area, and the weathered B-horizon looks very similar. The C-horizon makes the distinction for the different soils, some are lapilli layers with a buried Bb-horizon beneath and others are loose dark grey sand layers.

Lf312, Lower glacis of the step-faulted plateau

Only one observation is made in this map unit, as there are no signs of wind erosion at this side of the study area. It has a gently undulating slope of 2 to 5%. The soils are generally deep and also somewhat excessively drained. Dark greyish (10YR4/2) or olive brown (5Y5/2) loamy sands with a weak to moderate structure in the B-horizon with a pH around 4.5. The C-horizon has a grey colour (5Y6/1), sand with a very weak structure, pH around 5. Below this a lapilli layer is found. Vegetation is also grassland with extensive grazing and more small farms are found in this unit. In this map unit only soil phase A is found.

Pv111, Very gently sloping, without dunes

Soils of this map unit are generally deep, somewhat excessively drained. Colour is olive brown (2,5Y4/3) or dark greyish brown (10YR4/2) when dry. The texture of the Bw or, when there is a C-horizon above the lapilli layer, is loamy sand. Structure is weak to moderate. pH is around 4.5 to 5.5. Beneath this horizon, a lapilli layer with abundant gravel is present, slightly weathered and probably deposited in two different epochs. Colours vary between greyish brown (2.5Y5/2) and yellowish brown (2.5Y6/4). Texture is sandy clay and pH. Below this lapilli layer a buried soil is found with a colour range of brown (10YR4/3) to very dark brown (10YR2/2). Texture is also sandy loam, with a weak (massive) structure. pH is 8 or 9 and with some evidence of calcium. Vegetation is mainly grassland with extensive grazing and a few scattered small farms (5 acres). Sand deposition areas are found in this map unit. Soil phases A en C are found in this unit, but soil phase A is the most common one. It is found higher up on the gently sloping plain. Soil phase C occurs more closely to the map unit Pv112, where very low dunes are present.

Pv112, Very gently sloping, with very low dunes (0.3 to 2.0 meters)

The soils in this map unit do have the same properties as the soils in map unit Pv111, but the micro-relief is more pronounced with very low dunes up to 2.0 meters. All three soil phases are present in this map unit. Soil phase A is present in the northern part of this map unit, and probably also in the southern part of it, although no observations has been made. Soil phase B can be found in deflation areas, whereas soil phase C are located near low dunes.

Pv113, Very gently sloping, with low dunes (2.0 to 4.0 meters)
Soils of this map unit are generally deep, somewhat excessively drained. The Bw-horizon is thick, around 70 cm and has an olive brown colour (2.5Y4/2) or (2.5Y4/3) when dry. Texture is loamy sand, and structure is weak. pH is around 4.5-5. Below this Bw-horizon several C-horizons are found, with a light olive brown (2.5Y5/3) or light brownish grey (2.5Y6/2) loamy sand with a weak structure covering a very dark (2.5Y3/2 or 2.5Y4/1) sandy soil with a loose structure. pH is around 7. Especially the dark sand layers are typical for this map unit. Deep below these C-horizons (more than 3 meters) again lapilli layers are present with underneath probably a buried soil. Vegetation is also grassland with extensive grazing, but there are no small farms situated in this unit. Micro-relief is even more pronounced with low dunes up to 4.0 meter. In this unit many deflation trenches are found. Soil phase C is very characteristic for this map unit.

1.4. Analysis of current wind erosion status

1.4.1. Mapping of wind erosion features

During the fieldwork a wind erosion feature survey was carried out based on the interpretation of the small format aerial photographs. The results are presented in Figure 10 and Table 10. Most of the deflation areas are found on the south-eastern site of the study area, whereas smaller deposition areas are found in the northern part of the area. Below the descriptions of the map units are given.

D - Deflation / abrasion areas (blow outs)
Different types of deflation trenches are found in the study area. They differ in shape, size, and nature of exposed layers. Size differs from very small ones of only a few square meters to big elongated trenches that cover relative big areas. The depth of the deflation trenches varies between 0.5 meter to 4.0 meter. Only one trench in the area has a depth of 4 meter (see Figure 11) and is also the only one that existed in 1991. The smaller deflation trenches (D1) do have only an exposed Bw-horizon, which gives a brownish colour on the photographs. Bigger trenches (D21) show also a C-horizon, which has a greyish black colour. Some deflation trenches (D22 and D23) show also light greyish spots, when ash layers are exposed to the surface. In some trenches, the floor is covered with small obsidian gravel that forms a desert pavement. Outside the study area, there are trenches where even the buried soils are exposed.

S - Depositional areas (blown sand sheets)
Depositional areas are found in the whole area. Most of them are associated with deflation trenches, others not. The thickness of these sand sheets is a good indicator to distinguish the three types in the area. The thinnest sand sheets (S1), less then 5-cm are found in different places. Tussock grasses are very good “sand-traps”, and areas with a relative good grass cover do contain depositions of sand. Small deflation areas do have sand deposition on most of the sides. These thin sand depositions have

Table 10. Wind erosion features (WEF) legend

API map unit	*Description*	*Source of soil material*
Areas affected by wind erosion		
D – Deflation / abrasion areas (blow outs)		
D1	Brown eroded Bw horizon (somewhat coherent loamy sand) exposed at surface	Bw- horizon
D21	Light-dark grey C- material consisting of loose fine to medium sandy volcanic ash exposed consisting sandy ash; deflation depth < 1.0 m.	C- , 2C or 3C horizon
D22	- do - but with deflation depth between 1.0 – 2.0 m	- do -
D23	- do - but with deflation depth > 2.0 m	- do -
S – Depositional areas (sand sheets)		
S1	Predominantly loose dark grey medium sandy ash ; sheet depth less 5 cm; not associated with rear-side of deflation trench	Mixed Bw and C-horizons
S21	- do – but depth of sand sheet between 5 – 25 cm; associated with rear-side of deflation trench	- do -
S22	- do – but depth of sand sheet > 25 cm; associated with rear-side of deflation trench	- do -
W – Areas affected by deposition from (water) erosion gully		
W1	Gully wash fan; light grey pumice gravel and scattered shrubs	Gully wash including pumice gravel from up-slope areas
W2	-do-; light yellowish brown soil (10YR6/4) with less than 25% dry grass stubble	Surface material
W3	Complex of W1 and W2	Combination of above
O – Other degraded areas		
O1	Light yellowish brown (2.5Y5/3) soil-crusted area (sealed as cattle residential area / dung collection	A- and Bw horizon
O2	Other degraded areas caused by other factors than wind or water. Most of them are caused by human influence, like small road cuts and disturbing soil by digging.	n.a.
N – Areas unaffected by wind erosion		
N	Level part of Pv with dry, relatively dense, light grey grass cover, not degraded.	n.a.

Figure 10. Wind erosion feature map

generally a more brownish colour, originated from the Bw- and some dark grey sand from the C-horizon. Other depositional areas are associated with the deflation trenches and are found at the rear side of these. Some of these areas are thick (S22), over 25 cm till more than 50 cm. It contains more sand from the dark greyish C-horizons than the brownish Bw-horizon. Remnant “pillars” of these Bw-horizons are visible in these depositions.

The movement of sand occurs in two directions. The general direction is from east to west, but there is also a lateral movement to the north (see Figure 14). This lateral movement however is less pronounced.

W - Areas affected by deposition from (water) erosion gully

On the eastern side of the area an extensive deposition area exist caused by water erosion. The origin lies on the other side of the road where before 1991 a dirt road is constructed. Between 1991 and 2000 the road is heavily eroded and formed a gully of more than 3 meters deep and 2 meters wide for a hundred metres long. The content of this gully is deposited in the study area. Some parts of the deposition consist of pumice gravel with scattered scrubs, other areas are covered with yellowish brown soil or combination of these two.

O - Other degraded areas

The study area is found between two hills (Mt. Longonot and Kijabe Hill), Maasai has to travel through this relatively narrow pass with their large herds. Around some farms (abandoned or not) these herds rest at night, what results in a sealed and compacted area caused by trampling. It has a typical yellowish brown colour. The dung of these animals is collected and piled up. Furthermore there are a few degraded areas due to a combination of water and wind erosion and road construction activities.

N - Areas unaffected by wind erosion

These are areas with an a more or less continuous natural cover of grass or woody shrubs (*Acacia spp.*) Also dunes are distinguished, very low dunes (0.3-2 metres) and low dunes (2-4 metre). However, in many places the grassland vegetation itself shows clear signs of deterioration due to overgrazing in combination with drought

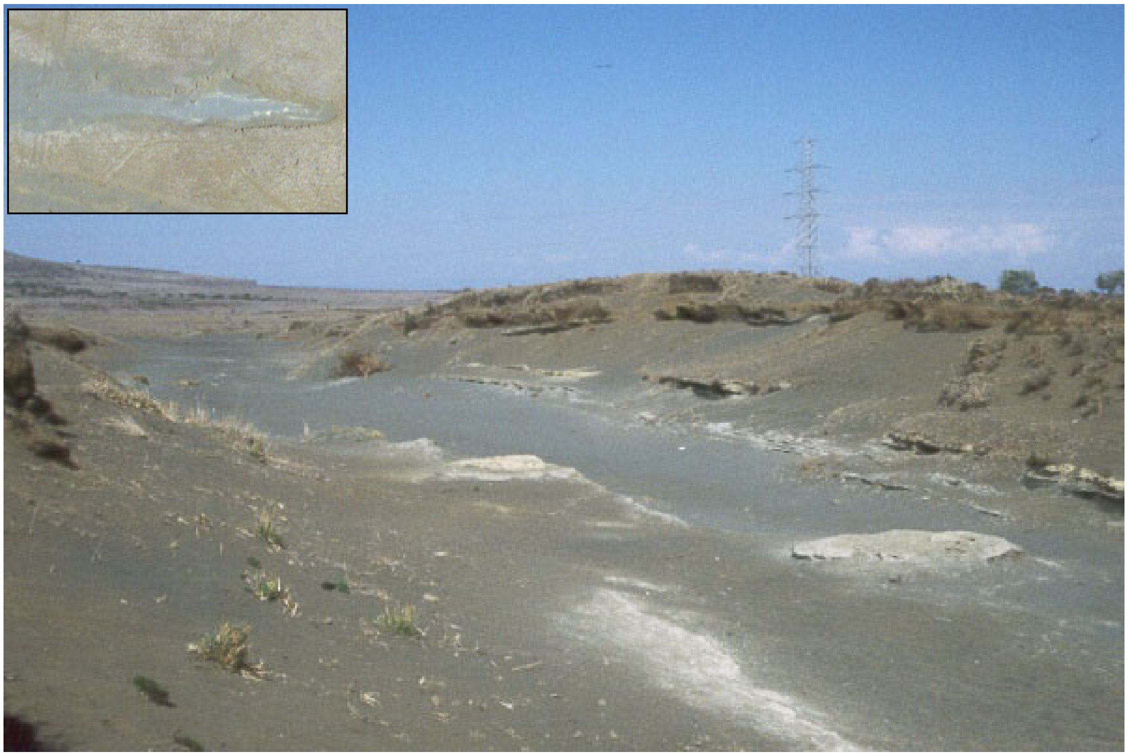

Figure 11. Deep deflation trench (map unit D23) in a low dune with dark grey sand and light grey ash layers exposed in the trench bottom and along sides . A SFAP image of the same area is inserted.

Figure 12. Old aeolian deposits consisting of laminated dark grey ash material overlying light grey ash material in the lower subsoil of soil profile NAIV/2000/AN/003 (soil phase C)

Figure 13. Coalescing deflation trenches form vast sand sheets of very erodible volcanic ash. These ash sheets show sand ripples, which are locally protected from the wind forces by the formation of a thin desert pavements

Figure 14. Sand ripples showing the influence of two different wind directions

Table 11. Extent of wind erosion features map units

Description	*Map unit*	*Number of delineation's*	*Size (ha)*	*Total (ha)*
D - Deflation /abrasion areas	D1	5	0.1	
	D21	18	0.3	
	D22	17	1.2	
	D23	1	0.2	
	Subtotal	*41*		*1.8*
S - Depositional areas	S1		3.6	
	S21	15	5.4	
	S22	6	10.0	
	Subtotal	*34*		*19.0*
W - Areas affected by water erosion	W1	1	0.7	
	W2	3	2.0	
	W3	2	3.1	
	Subtotal	*6*		*5.8*
O - Other degraded areas	O1	7	1.4	
	O2	4	0.6	
	Subtotal	*11*		*2.0*
N - Areas unaffected by wind erosion	N	-	284.3	
	Subtotal			*284.3*
Farmland	Subtotal			57.7
Total		118		370.6

1.4.2. Interpreting and classifying wind erosion severity

a) Degree of present degradation

The degree of present degradation reflects the intensity of degradation at a particular site. GLASOD presents an overview of the degree of present degradation due to wind erosion (Oldeman, 1997). For the study area, degradation degree classes has been identified and differentiated according the land degradation type.

D - Deflation areas

None: There is no visible sign of present degradation.

Slight: The topsoil is partly removed, exposing the brown Bw-horizon. The depth of the degraded areas is less than 1 metre. This corresponds with the D1 map unit in the WEF- legend.

Moderate: The topsoil is completely removed and the dark grey C-horizon is exposed. Depth of the deflation areas is in general around 1 meters. These are deflation trenches classified as D21 in the WEF-legend.

Severe: The topsoil is completely removed. The C-horizon is exposed with light grey ash-layers and dark grey sand layers. Depth varies from 2 to 4 meters. In the WEF-legend classified as D22 and D23 features.

S - *Deposition areas*

None: There is no visible sign of present deposition.

Slight: Areas were the deposition is less than 5 cm, some grasses are still present. This corresponds with the S1 map unit of the WEF-legend.

Moderate: Areas with a thicker deposition between 5 and 25 cm, corresponding with the S21 map unit of the WEF-legend.

Severe: Areas with a deposition thickness of more than 25 cm, corresponding with the S22 map unit of the WEF-legend.

W *Degradation caused by water erosion*

None: There is no visible sign of degraded areas caused by water erosion.

Slight: Rills caused by water erosion, not seen in the area.

Moderate: Deposition of sand and pumice by water, in a thin layer. Corresponding with the W2 and W3 map unit of the WEF-legend.

Severe: Deposition of sand and pumice by water, in a relatively thick layer. This class corresponds with the W1 classification of the WEF –legend.

O *Other degraded areas*

None: There is no visible sign of other degradation

Slight: Areas with a sealed or crusted surface, caused by cattle trampling. This corresponds with the O1 map unit of the WEF-legend. Also other small, degraded areas with no known cause are included in this class.

b) *Extent of soil degradation*

In addition to the degree of present degradation, the spatial extent in a particular area is important. This is expressed as the frequency of occurrence within the delineated mapping unit. Table 12 presents the extent of soil degradation according the following five classes which is also used in the GLASOD methodology (Oldeman, Lynden et al. 1997):

Infrequent: Up to 5% of the map unit is affected
Common: 6 to 10% of the map unit is affected
Frequent: 11 to 25% of the map unit is affected
Very frequent: 26 to 50% of the map unit is affected
Dominant: Over 50% of the map unit is affected

Table 12. Extent of soil degradation per geopedological map unit

Geopedological map unit	*Area (m2)*	*Degraded area (m2)*	*% degraded area per map unit*	*Degraded area by water erosion (m2)*	*% degraded area by water erosion per map unit*	*Frequency of occurring*
Lf311	65,740	900	1.4			Infrequent
Lf312	465,890	21,690	4.7	10,600	2.3	Infrequent
Lf411	104,860	460	0.4			Infrequent
Pv111	901,910	48,990	5.4	45,590	5.1	Infrequent
Pv112	1,206,560	92,400	7.7	1,130	0.1	Common
Pv113	863,190	120,950	14.0			Frequent

c) Severity of soil degradation

To obtain the severity of soil degradation for the area, a matrix (Table 13) is constructed which is based on the combination of a) degradation degree and b) degradation frequency classes (adapted from Oldeman 1997).

Table 13. Soil degradation severity classes

Degree of soil degradation:	*Frequency of soil degradation*				
	Infrequent	*Common*	*Frequent*	*Very frequent*	*Dominant*
Slight	Slight	Slight	Medium	Medium	High
Moderate	Medium	High	High	Very high	Very high
Severe	Medium	High	Very high	Very high	Very high

Table 14 and Figure 15 presents the result of above process. The severity classes are subdivided according the geopedological map units. Figure 16 presents the spatial pattern of the severity of current land degradation in the study area.

Table 14. Severity classes and their percentage per geopedological map unit

	Severity Class									
	None		*Slight*		*Medium*		*High*		*Very high*	
	Area (m^2)	*%*	*Area(m^2)*	*%*	*Area(m^2)*	*%*	*Area(m^2)*	*%*	*Area(m^2)*	*%*
Lf311	65,650	99.9	90	0.1	-		-		-	
Lf312	444,190	95.1	4,890	1.1	16,810	3.8	-		-	
Lf411	104,400	99.6	420	0.4	40	0.0	-		-	
Pv111	852,930	94.5	580	0.1	48,400	5.4	-		-	
Pv112	1,114,160	92.3	37,310	3.1	-		55,090	4.6	-	
Pv113	753,580	87.3	-		1,260	0.1	40,180	4.7	68,170	7.9
Total	3,334,910	92.4	43,290	1.2	66,510	1.8	95,270	2.6	68,170	1.9

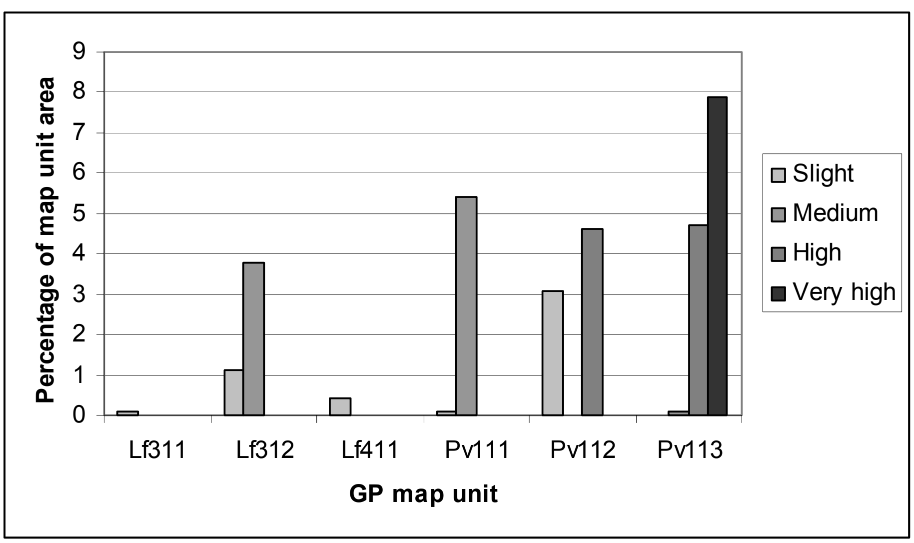

Figure 15. Severity classes and their percentage per geopedological map unit

Of the degraded area 16% falls in the severity class “slight”, 24% in “medium”, 35% in “high” and 25% in “very high”.

Lf311 Upper part of glacis
Almost no land degradation is found in this map unit.

Lf312 Lower part of glacis
Around 5% of this map unit fall in the severity classes slight and medium. Water erosion is the dominant factor for land degradation in this map unit

Lf411 Alluvial fan
Almost no land degradation is found in this map unit.

Pv111 Plain, very gently sloping
Around 5 ha of the Volcanic Plain without micro-relief falls in the severity class medium. Some depositional areas (S21, S22) and deflation areas (D21, D22) are found, but again water erosion is the most dominant factor for this class.

Pv112 Plain, very gently sloping with very low dunes
Around 8% of this map unit is degraded, of which 3.7 ha confines to the severity class slight and 5.5 ha to the severity class high. This last class is predominantly caused by deep sand depositions (S1, S21 and S22), and most of the smaller deflation trenches (D1, D21 and D22). The classes “slight” consists of degradation caused by cattle trampling (O1) and thin sand deposition areas (S1). Water erosion is almost absent.

Pv113 Plain, very gently sloping with low dunes
In this map unit, severity classes medium, high and very high are found. More than 12% (11 ha) of the area falls in these severity classes. All the bigger deflation trenches (D21, D22 and D23) are found in this unit and are classified as very high severity. Thick sand depositions (S22) are also included in this class.

Figure 16. Severity of current land degradation in the study area, largely due to wind erosion

1.5. Spatio-temporal analysis of wind erosion

1.5.1. Trends and approximate rate of wind erosion

One of the objectives of this study is to obtain information on trend and approximate rate of wind erosion in the study area. This requires first a general analysis of surface area and volumetric loses in the study area.

a) Surface area loss

The aerial photographs of 1991, shows only one large deflation trench with a deposition area at the rear of it. Furthermore, some very small, degraded areas could be distinguished on the photograph. The total degraded area does not exceed 1.4 ha. In 2000, however, the total degraded area has increased to 28.5 ha, what means a twenty-fold increase. Also, the number of deflation trenches has increased sharply in those nine years.

Table 15 presents an overview of the increase in area of deflation trenches per geopedological map unit in the period 1991-2000, whereas Table 16 presents data of deflation and deposition for the whole study area.

Table 15. Change in deflation areas in the period 1991-2000

WEF	*D1*				*D21*				*D22*				*D23*			
Year	1991		2000		1991		2000		1991		2000		1991		2000	
m^2	Area	%	Area	%	Area	%	Area	%	Area	%	Area	%	Area	%	Area	%
Lf312	-		-		-		400	0.6	-		-		-		-	
Pv111	-		-		-		30	0.0	-		400	0.0	-		-	
Pv112	-		-		-		930	0.1	-		160	0.0	-		-	
Pv113	-		1,230	0.1	-		1,760	0.2	2,150	0.2	11,400	1.3	-		2,540	0.3

Table 16. Changes in deflation and deposition areas in the period 1991-2000

Year	*1991*		*2000*	
	Area (m^2)	*% of study area*	*Area (m^2)*	*% of study area*
D - Deflation area	2,150	0.05	18,850	0.5
S - Deposition area	11,430	0.3	190,000	5.3

The large deflation trench visible on the 1991 aerial photograph has increased with around 400 m^2 to more then 2,500 m^2. The total deflated area has increased ten-fold, from 0.2 ha (0.05%) to 1.9 (ha) 0.5% of the study area. This corresponds with an annual increase of 0.2 ha/yr.

The amount of material eroded from these trenches has partly taken from the area by the wind, but an important part is deposited as sand sheets in the area itself. The area covered by sand depositions has also increased from 1.1 ha (0.3%) to 19 ha (5.3%). This corresponds with 2.0 ha/yr.

It should be remarked that farmers have indicated that serious wind erosion involving the formation of deflation trenches and sand deposits did not really start until 1995-'96 (Ataya 2000). This would mean that the rate of expansion during the past 5 years is probably much higher than the rate calculated over the last nine years and that this rate is likely to accelerate.

b) Rate of soil loss

Losses from deflation trenches are generally difficult to estimate because most of the trenches have different, irregular forms. Some cut through low dune fields with clearly domed crests (see Figure 11) whereas other trenches occur in more level terrain. Again other trenches appear more like round depressions. Also, sides of trenches may vary: some are almost vertical while others tend to be more inclined.

Yet, an attempt has been made to estimate current soil losses and soil loss rates using a simple model. During fieldwork, the depth of the different deflation trenches is estimated and grouped in depth classes of 0.5m. 8 depth classes have been identified as follows: 0-0.5m, 0.5-1.0m, etc.

To estimate the average depth of a deflation trench two different approaches are followed:

1) Minimum of the depth class is taken (e.g. 1m for 1-1.5m class), except for the first class (0-0.5m) where 0.25m is taken.
2) Mean depth is taken for each class (e.g. 1.25m for 1-1.5m class)

The volume loss can be calculated, as the area and depth class of each deflation trench is known. The results of this soil loss calculation are presented in Table 17.

Table 17. Estimated soil loss per geopedological map unit in the period 1991-2000

	Volumetric soil loss		*Weight soil loss*	
	m^3/ha	*m^3/ha/year*	*Tons/ha*	*Tons/ha/year*
Lf311	0	0	0	0
Lf312	2	0.2	2.6	0.3
Lf411	0	0	0	0
Pv111	17 – 21	1.9 – 2.3	22 – 27	2 – 3
Pv112	3 – 4	0.3 – 0.4	4 –5	0.4 – 0.5
Pv113	200 – 240	22 – 27	260 – 310	29 – 34
Total	**53 – 64**	**6 – 7**	**69 – 83**	**8 – 9**

The estimation of the soil loss in map unit Pv113 is corrected for the data of 1991, although soil loss estimate from the deflation trench in 1991 is difficult as the depth is unknown. Presumably the average depth is around 2.5 meter, giving a loss of 5,400 m^3. Volumetric soil loss in this map unit is around 200-240 m^3/ha. Over the last 9 years the volumetric soil loss is 22 – 27 m^3/ha/year.

The estimated volumetric losses in the study area caused by wind erosion vary between 24,600 and 28,500 m^3. The average bulk density of the soils in the area is estimated at 1.3 ton/m3. That gives a total of 32,000 to 37,100 tons of soil that is lost.

In the study area, there is a strong relation between deflation areas and the deposition areas, as the latter almost always occur at the rear-side of the deflation trenches. To verify if the estimation of depth of deflation trenches is acceptable, the area covered by blown sand is calculated. This calculation is merely done to verify it the volumetric losses estimations have not been over-estimated. As the thickness of the deposition layers is in general around 25 cm, an area of 10 to 11.5 ha can be covered by the amount blown out from the deflation trenches. This corresponds quite well with the area of 15.4 ha that is covered by S21 and S22 depositions. It should be noted in this respect that a) part of the sand deposited is allochthonous i.e. blown in from outside the study area and that b) part of the autochthonous sand i.e. coming from the deflation area within the study area is moved out of the area (in creep, saltation or suspension mode).

1.5.2. Analysis of relationship wind erosion with underlying erosion factors

a) Influence of micro-relief and soil-related factors

Micro-relief and soil are two key factors in the wind erosion process in the study area. As explained in Chapter 2 on low dunes with slopes of more than 1.5% the lines of equal wind velocity are compressed giving a higher wind drag speed. Also, the length of such a dune slope is important, as lines of equal wind velocity tend to follow the contour of the land when the length of these dunes exceed a certain distance. In the study area, the general maximum slope of low dunes is around 5-6% and the length of these dunes is less than 200 meters. When the wind hits the low dunes in the study area the wind drag speed will increase in such a way that sand particles are easily moved.

Moving the sand particles depends on the erodibility of the soil. Looking at Table 17, map unit Pv113 has the highest soil loss per ha. The soil in this map unit belongs to soil phase C (see Table 9), which has a loose, highly erodible subsoil below its Bw-horizon. The other two map units in the Volcanic Plain do have other soils that belongs to soil phase A, which lacks this highly erodible subsoil below its Bw-horizon. This explains why wind erosion in map unit Pv111 and Pv112 is not as severe as in map unit Pv113.

Before the wind can reach the dark grey sand layer and start the subsoil erosion, first the structure of the Bw-horizon has to be destroyed. The explanation for this will be given in the following paragraph.

b) Influence of current and previous land use

For this analysis the aerial photograph of 1991 and SFAP's of 2000 are used to obtain two maps of land use and relate the differences with wind erosion occurring in the area.

Figure 17 gives an impression of the land use changes from 1991 to 2000.

The history as described in paragraph 3.4 is clearly visible in this figure. In 1991 around 94 farms or arable fields were present, covering around 145 ha (40% of the pilot study area). The majority of these farms were located on the east-side of the area, but arable fields were also present at the west-side. In 2000, only 43 farms or arable fields were still present, covering around 57 ha (15% of the pilot study area). This is a reduction of more than 50% in farms and 60% in land cover. Only three farms have started or have extended their fields after 1991. During fieldwork, which was carried out after a very dry year, only fenced farms were observed. Especially at the western side of the area farms and fields were abandoned. This is also the area were severe land degradation is occurring, caused by wind erosion.

Table 18. Land use change 1991 - 2000

Land use	*1991*			*2000*		
	Number of delineation's	*Area (ha)*	*% of study area*	*Number of delineation's*	*Area (ha)*	*% of study area*
Arable field	94	145	40	43	57	15
Rangeland and roads / tracks	1	135	60	1	313	85

Figure 17 gives a good explanation why so much arable fields are abandoned and why wind erosion has accelerated the last 9 years.

- In total 41 deflation trenches were found in the area during fieldwork. 18 of these deflation trenches, including the larger ones, are located on sites where under arable farming in 1991, but were abandoned in 2000.
- All abandoned fields, where deflation trenches were found in 2000, are situated in the map unit Pv113 (Volcanic Plain with low dunes complex).
- Furthermore 7 deflation trenches were found along (old) farm roads and field boundaries.

Figure 17. Land use change 1991-2000

1.6. Cost and labour aspects

One of the research questions is what does it cost in money and labour, and what is the time required to have a final product? Table 19 gives an overview of the time and money needed for the different steps to obtain a current status map of wind erosion of the area.

Table 19. Cost and labour of flight and fieldwork

	Number of working days	*Cost US$)*
Flight preparation	1.0	
Films		20
Execution of flight	0.5	220
Developing photographs	1.0	40
Interpretation of photographs (14)	2.0	
Collecting of GPS points (180)	3.0	
Collecting wind erosion data	2.0	
Scanning photographs	0.5	
Georeferencing photographs	1.0	
Digitizing and compilation of final map	2.0	
Total	**13.0**	**280**

In total, 13 working days are needed to cover an area of around 370 ha, 2.5 days for flight preparation and obtaining the photographs, 5 days of fieldwork and 5.5 days office work.
This does not imply that it can be done in two weeks. Between planning the flight and the actual making of the flight, several days can be lost because of poor, cloudy weather conditions. During this fieldwork period, almost two weeks were lost exactly due to such circumstances. However, SFAP compares very favourably with conventional aerial photography where only in exceptional cases such a short delivery time can be achieved.

Compared with conventionalaerial photographs, the cost of the SFAP flight is minimal. For the reconnaissance and study area (15.3 km^2, scale 1:5,000), less than US$ 20 per km^2.Comparing this with for instance an urban cadastral project in Bolivia with a comparable scale (1:4,000), costs were around US$ 300 per km^2.

The cost of manpower is not calculated, as the cost of wages is not known. But comparing it again with normal aerial photography, most of the time is spent in the field and office and that will not change much.

1 Conclusions and recommendations

1.1 Conclusions

In the research problem the general lack of up-to-date information about the area was mentioned is the major constraint to the proper analysis of wind erosion, this research was helpful in obtaining relevant and up-to date information about the status of wind erosion.

a) General conclusion

- The use of SFAP generally proved to be quite promising in analysing and assessing the current status and trends of wind erosion as occurring in Naivasha, a dry sub-humid volcanic area in the central Rift Valley of Kenya.

The following conclusions form the basis for the general conclusion.

b) Generation and rectification of SFAP

- An adequate large-scale SFAP cover (scale 1: 5,000 of the printouts) of a selected pilot area (370 ha) could be achieved within a relatively short time (2 weeks).

- Main operational constraints included (a) adverse weather conditions prior to flying (cloudiness) and during the flight (wind gusts) the latter in combination with the low speed as required and the low weight of the aircraft itself.

- The visual quality of the SFAP generally ranges from good to excellent allowing for rapid detection and detailed analysis of wind erosion features and other land degradation-related phenomena. Height differences of down to 1 m appear to be readily detectable on the SFAP image.

- The major advantage of SFAP over conventional aerial photography as far as photo image quality is concerned is its effective combination of (a) large photo scale, (b) acceptable sharpness of the photo image - though admittedly less than for conventional photography - (c) a (highly informative) photo colour and, last but not least (d) very recent photo date. Above factors combined allow for detailed and accurate photo-interpretation followed by field checking including rapid field orientation and feature detection.

- For the rectification of SFAP three different transformation methods were applied; (a) direct linear transformation, (b) projective transformation and (c) orthophoto. From the results of the direct linear transformation it could be concluded that the study area is a flat area. Therefore correction for relief displacement is not necessary and the projective transformation can be used.

- The aerial photograph (1:20,000) was rectified with the projective transformation, using the same ground control points (GPS observations) as for SFAP. Information from this aerial photograph like geomorphology, infrastructure and land use could be satisfactorily combined with the corresponding information of the SFAP's.

c) Soils and landscape in the study area.

- The soils in the study area classified as Areno-Vitric Andosols (Dystic) according WRB. This classification takes only in account the upper parts of a soil profile, in this case a relatively thick Bw-horizon with a low erodibility. This classification is not useful as the sub-soils have completely different properties regarding erodibility. Therefore three soil phases are distinguished to include the properties of the subsoil (C-horizons). Soil phase A has a low subsoil erodibility due to a lapilli layer, and soil phase C has a high subsoil erodibility due to sand and ash layers in the C-horizons, whereas soil phase B is typical for deposition areas.

d) Analysing of current wind erosion status.

- Using the method as being described in the research method (Chapter 4.1) it is possible to use SFAP as a complement to conventional aerial photographs.

- After crossing the geopedological map with the wind erosion current status map, it can be concluded that the majority of the deflation trenches are found in the geopedological map unit Pv113, Volcanic plain, very gently sloping (1-%) with low dunes (2-4m), with soils belonging to soil phase C.

- Two major types of wind erosion features could be distinguished: Deflation / abrasion trenches (0.5%) and Deposition areas or sand sheets (5.3%). Other degraded areas included those affected by water erosion (1.6%) and miscellaneous erosion types (0.6%). 71.4% of the study area is not affected by erosion or deposition of any kind.

- With respect tot current status of wind erosion, 4.5 % of the study area appears to be severely to very severely degraded by wind erosion, 3.0 % is slightly to moderately degraded and 92,5% is non-degraded. For map unit Pv113 which comprises the most affected and most erodible part of the study area these values are 12.6 %, 0.1% and 87.3 %, respectively.

- Total and annual (volumetric) soil losses per ha in the area appear to be in the range of 53 – 64 m^3/ha and 6-7 m^3/ha/year, respectively. Assuming an average bulk density of 1.3 tons/m^3, total and annual weight losses from the area are estimated at 69-83 tons/ha and 8-9 tons/ha/year, respectively. For map unit Pv113 total and annual weight losses are in the range of 260 – 310 tons/ha and 29-34 tons/ha/year, respectively

e) Spatio-temporal analysis of wind erosion.

- Human activities have induced this wind erosion process as the topsoil of the low dunes does have a low erodibility. The land use map of 1991 reveals that almost all large deflation trenches are found on old agricultural field which were abandoned afterwards. Land preparation has destroyed the protective top-layer and subsoil wind erosion could start. Also roads and tracks have accelerated this process.

1.2 Recommendation

Although a general insight in the nature and current status of wind erosion and underlying factors has been obtained, many questions remain. To answer these questions additional climatic data are required, especially on wind speed and direction.

Research to the origin, formation and effect of the old low dune fields in the western part of the area has to be undertaken in order to obtain a better understanding of the micro-topographic and soil factors in the current wind erosion process in the area.

Immediate action has to be taken to protect the area against further degradation by wind erosion. However, such action should be taken with full participation of local stakeholders including pastoralists, farmers and NGO's such as Naivasha Riparian Owner Association.

Further research has to be done on the performance of SFAP in combination with GPS (GARMIN 12). Especially, the propagation of error (or partly correction by rectifying) will be a very interesting study.

1 Conclusions and recommendations

1.1 Conclusions

In the research problem the general lack of up-to-date information about the area was mentioned is the major constraint to the proper analysis of wind erosion, this research was helpful in obtaining relevant and up-to date information about the status of wind erosion.

a) General conclusion

- The use of SFAP generally proved to be quite promising in analysing and assessing the current status and trends of wind erosion as occurring in Naivasha, a dry sub-humid volcanic area in the central Rift Valley of Kenya.

The following conclusions form the basis for the general conclusion.

b) Generation and rectification of SFAP

- An adequate large-scale SFAP cover (scale 1: 5,000 of the printouts) of a selected pilot area (370 ha) could be achieved within a relatively short time (2 weeks).

- Main operational constraints included (a) adverse weather conditions prior to flying (cloudiness) and during the flight (wind gusts) the latter in combination with the low speed as required and the low weight of the aircraft itself.

- The visual quality of the SFAP generally ranges from good to excellent allowing for rapid detection and detailed analysis of wind erosion features and other land degradation-related phenomena. Height differences of down to 1 m appear to be readily detectable on the SFAP image.

- The major advantage of SFAP over conventional aerial photography as far as photo image quality is concerned is its effective combination of (a) large photo scale, (b) acceptable sharpness of the photo image - though admittedly less than for conventional photography - (c) a (highly informative) photo colour and, last but not least (d) very recent photo date. Above factors combined allow for detailed and accurate photo-interpretation followed by field checking including rapid field orientation and feature detection.

- For the rectification of SFAP three different transformation methods were applied; (a) direct linear transformation, (b) projective transformation and (c) orthophoto. From the results of the direct linear transformation it could be concluded that the study area is a flat area. Therefore correction for relief displacement is not necessary and the projective transformation can be used.

- The aerial photograph (1:20,000) was rectified with the projective transformation, using the same ground control points (GPS observations) as for SFAP. Information from this aerial photograph like geomorphology, infrastructure and land use could be satisfactorily combined with the corresponding information of the SFAP's.

c) Soils and landscape in the study area.

- The soils in the study area classified as Areno-Vitric Andosols (Dystic) according WRB. This classification takes only in account the upper parts of a soil profile, in this case a relatively thick Bw-horizon with a low erodibility. This classification is not useful as the sub-soils have completely different properties regarding erodibility. Therefore three soil phases are distinguished to include the properties of the subsoil (C-horizons). Soil phase A has a low subsoil erodibility due to a lapilli layer, and soil phase C has a high subsoil erodibility due to sand and ash layers in the C-horizons, whereas soil phase B is typical for deposition areas.

d) Analysing of current wind erosion status.

- Using the method as being described in the research method (Chapter 4.1) it is possible to use SFAP as a complement to conventional aerial photographs.

- After crossing the geopedological map with the wind erosion current status map, it can be concluded that the majority of the deflation trenches are found in the geopedological map unit Pv113, Volcanic plain, very gently sloping (1-%) with low dunes (2-4m), with soils belonging to soil phase C.

- Two major types of wind erosion features could be distinguished: Deflation / abrasion trenches (0.5%) and Deposition areas or sand sheets (5.3%). Other degraded areas included those affected by water erosion (1.6%) and miscellaneous erosion types (0.6%). 71.4% of the study area is not affected by erosion or deposition of any kind.

- With respect tot current status of wind erosion, 4.5 % of the study area appears to be severely to very severely degraded by wind erosion, 3.0 % is slightly to moderately degraded and 92,5% is non-degraded. For map unit Pv113 which comprises the most affected and most erodible part of the study area these values are 12.6 %, 0.1% and 87.3 %, respectively.

- Total and annual (volumetric) soil losses per ha in the area appear to be in the range of 53 – 64 m^3/ha and 6-7 m^3/ha/year, respectively. Assuming an average bulk density of 1.3 tons/m^3, total and annual weight losses from the area are estimated at 69-83 tons/ha and 8-9 tons/ha/year, respectively. For map unit Pv113 total and annual weight losses are in the range of 260 – 310 tons/ha and 29-34 tons/ha/year, respectively

e) Spatio-temporal analysis of wind erosion.

- Human activities have induced this wind erosion process as the topsoil of the low dunes does have a low erodibility. The land use map of 1991 reveals that almost all large deflation trenches are found on old agricultural field which were abandoned afterwards. Land preparation has destroyed the protective top-layer and subsoil wind erosion could start. Also roads and tracks have accelerated this process.

1.2 Recommendation

Although a general insight in the nature and current status of wind erosion and underlying factors has been obtained, many questions remain. To answer these questions additional climatic data are required, especially on wind speed and direction.

Research to the origin, formation and effect of the old low dune fields in the western part of the area has to be undertaken in order to obtain a better understanding of the micro-topographic and soil factors in the current wind erosion process in the area.

Immediate action has to be taken to protect the area against further degradation by wind erosion. However, such action should be taken with full participation of local stakeholders including pastoralists, farmers and NGO's such as Naivasha Riparian Owner Association.

Further research has to be done on the performance of SFAP in combination with GPS (GARMIN 12). Especially, the propagation of error (or partly correction by rectifying) will be a very interesting study.

Annex

Soil profile NAIV/2000/AN/001

A) Information on soil profile site.

Date of examination	26th September 2000.
Authors	Hennemann G.R., Nagelhout A.
Location	219313, 9903613 (UTM, ARC1960). Longonot, Naivasha area.
Elevation	2,126 meter above sea level.
Geopedological unit	Pv113 Volcanic plain , very gently sloping (0-3%) with low dunes
Slope	Very gently sloping (0-3%)
Micro-topography	Profile site on crest of low dune (height 1.5-2.0m).
Vegetation	Degraded Thorn Acacia savannah (40-80% grass cover) with low scattered shrubs (*Acacia spp.*).
Land use	Extensive grazing by Maasai and isolated small farms (remnants of the Marula Settlement Scheme).

B) General information on the soil profile

Classification (WRB)	Areno-VitricAndosols (Dystric)
Parent material	Longonot ash (Lp8) and Akira pumice (Lpa).
Drainage class	Somewhat excessively drained
Internal drainage	Never saturated, well drained.
External drainage	Neither receiving nor shedding water.
Depth of ground water table	Below 3 metre.
Surface stones	None
Rock outcrops	None
Evidence of erosion	Very severe wind erosion. The profile is located in one of the sides of a wind erosion deflation trench. More than 50% of surrounding area is affected.
Human influence	Vegetation is strongly disturbed due to overgrazing and wind erosion.

.

C) Soil profile description

Photo	Ho-rizon	Depth (cm)	Description
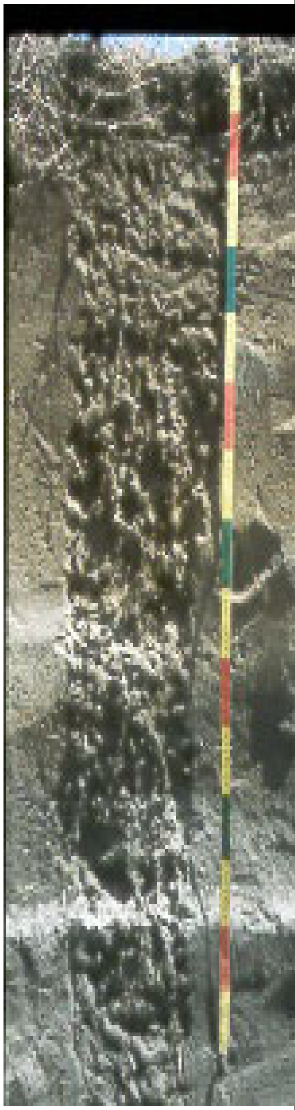	Ah	0-12	Dark greyish brown (2.5Y4/2) when dry, sand (medium sand); weak, medium subangular blocky; soft when dry; non sticky and non plastic when wet; many very fine, interstitial pores; few fine and common very fine roots; pH 5.
	Bw	12-79	Olive brown (2.5Y4/3) when dry and very dark brown (10YR2/2) when moist , loamy sand; weak, medium to coarse sub-angular blocky; soft to slightly hard when dry; non sticky and non plastic when wet; many very fine, interstitial pores; very few fine and few very fine roots; krotovinas; pH 4.5
	C	79-91	Light olive brown (2.5Y5/3) when dry and olive grey (5Y4/2) when moist, loamy sand; weak, medium to coarse sub-angular blocky; soft to slightly hard when dry; non sticky and non plastic when wet; many very fine, interstitial pores; very few very fine roots; pH 5.
	2C	91-126	Very dark greyish brown (2.5Y3/2) when dry and black (2.5Y2.5/1) when moist, sand; loose, single grain structure; loose when dry; non sticky and non plastic when wet; many very fine, interstitial pores; pH 6.5
	3C	126-132	Light brownish grey (2.5Y6/2) when dry and olive grey (5Y4/2) when moist, loamy sand; loose, single grain structure; soft when dry; non sticky and non plastic when wet; many very fine, interstitial pores; pH 7
	4C	132-170	Dark grey (2.5Y4/1) when dry and very dark grey (2.5Y3/1) when moist, sand; loose, single grain structure; loose when dry; non sticky and non plastic when wet; many very fine, interstitial pores; pH 6.5
	5C	170-180+	Dark olive grey (5Y3/2) when moist, sand; loose, single grain structure; very friable when wet; non sticky and non plastic when wet; many very fine, interstitial pores; pH 7

Remark: Deeper subsoil below 180 cm shows continuation of 5C horizon followed by pumice gravel layer at 3 m depth (augering)

D) Laboratory data: Not available

Soil profile NAIV/2000/AN/002

A) Information on soil profile site.

Date of examination	27th September 2000.
Authors	Hennemann G.R., Nagelhout A.
Location	219470, 9903703 (UTM, ARC1960). Longonot, Naivasha area.
Elevation	2,130 meter above sea level.
Geopedological unit	Pv111 Volcanic Plain, very gently sloping (1-3%)
Slope	Very gently sloping (1-3%)
Micro-topography	Flat.
Vegetation	Degraded Thorn Acacia savannah (40-80% grass cover) with low scattered shrubs (*Acacia spp.*).
Land use	Extensive grazing by Maasai and isolated small farms (remnants of the Marula Settlement Scheme).

B) General information on the soil profile.

Classification (WRB)	Areno-Vitric Andosols (Dystric)
Parent material	Longonot ash (Lp8) and Akira pumice (Lpa).
Drainage class	Somewhat excessively drained.
Internal drainage	Never saturated, well drained.
External drainage	Neither receiving nor shedding water.
Depth of ground water table	Below 1.10 meter.
Surface stones	None
Rock outcrops	None
Evidence of erosion	No erosion
Human influence	Vegetation strongly degraded due to overgrazing.

C) Soil profile description

Photo	Horizon	Depth (cm)	Description
	Bw	0-43	Olive brown (2.5Y4/3) when dry and very dark greyish brown (10YR3/2) when moist, loamy sand; weak to moderate, medium to coarse sub angular blocky; soft when dry; non sticky and slightly plastic when wet; very few, very fine interstitial pores; few very fine and very few fine roots; pH 4.5 (lower part) to 5 (upper part).
	C	43-69	Olive grey (5Y5/2) when dry and olive grey 5y(4/2) when moist, loamy sand; weak, medium to coarse sub angular blocky; soft when dry; non sticky and non plastic when wet; very few fine gravel with angular shape, fresh or slightly weathered (pumice); very few, fine interstitial pores; few very fine roots; pH 5.5
	2C	69-81	Greyish brown (2.5Y5/2) when dry, gravely sandy clay; non sticky and non plastic; abundant medium gravel and common fine gravel, both angular shape and fresh or slightly weathered (Akira) pumice; few very fine roots.
	3C	81-108	Light yellowish brown (2.5Y6/4) when dry, gravely sandy clay; non-sticky and non plastic; abundant medium gravel and very few fine gravel, both angular shape and fresh or slightly weathered (Akira) pumice; pH 6.
	4Bb	108-170+	Brown (10YR4/3) when dry (upper part) and black (10YR2/1) when moist, dark yellowish brown (10YR2/1) when dry (lower part), sandy loam; weak, coarse subangular blocky; slightly hard when dry; non sticky and non plastic when wet; no rock fragments in the upper part, in the lower part many fine and medium gravel, both angular weathered (Akira) pumice; pH 8

D) Laboratory data: Not available

Soil profile NAIV/2000/AN/003

A) Information on soil profile site.

Date of examination	2th October 2000.
Authors	Nagelhout A.
Location	219147, 9903397 (UTM, ARC1960) Longonot, Naivasha area.
Elevation	2,127 meter above sea level.
Geopedological unit	Pv113, Volcanic Plain, very gently sloping (0-3%) with low dunes
Slope	Very gently sloping (0-3%)
Micro-topography	Low dunes
Vegetation	Degraded Thorn Acacia savannah (40-80% grass cover) with low scattered shrubs (*Acacia spp.*).
Land use	Extensive grazing by Maasai and isolated small farms (remnants of the Marula Settlement Scheme).

B) General information on the soil profile.

Classification (WRB)	Areno-VitricAndosols (Dystric)
Parent material	Longonot ash (Lp8) and Akira pumice (Lpa).
Drainage class	Somewhat excessively drained
Internal drainage	Never saturated, well drained.
External drainage	Neither receiving nor shedding water.
Depth of ground water table	Below 1.52 meter.
Surface stones	None
Rock outcrops	None
Evidence of erosion	Very severe wind erosion. The profile is at the windward side of a wind erosion deflation trench. Area more than 50% affected
Human influence	Vegetation strongly disturbed due to overgrazing.

C) Soil profile description

Photo	Ho-rizon	Depth (cm)	Description
	Bw1	0-53	Olive brown (2.5Y4/3) when dry, loamy sand; weak to moderate, medium to coarse sub angular blocky; soft when dry; non sticky and slightly plastic when wet; many very fine, interstitial pores; very few very fine and few fine roots; pH 5
	Bw2	53-72	Olive brown (2.5Y4/3) loamy sand; weak, medium to fine subangular blocky; soft when dry; non sticky and slightly plastic when wet; many very fine, interstitial pores; very few very fine roots; pH 5
	C	72-137	Light olive brown (2.5Y5/3) when dry sand; very weak and loose; loose when dry; non sticky and non plastic when wet; many very fine, interstitial pores; very few very fine roots; pH 6.5
	2C	137-147	Black (2.5Y2.5/1) when moist sand; weak and loose structure; loose when dry; non sticky and non plastic when wet ;many very fine, interstitial pores; pH 7
	3C	147-152+	Olive grey (5Y4/2) when moist sand; weak and loose structure; loose when dry; non sticky and non plastic when wet ; many very fine, interstitial pores; pH 6

D) Laboratory data: Not available

Soil profile NAIV/2000/AN/004

A) Information on soil profile site.

Date of examination	2th October 2000.
Authors	Nagelhout A.
Location	219087, 9904107 (UTM, ARC1960). Longonot, Naivasha area.
Elevation	2,119 meter above sea level.
Geopedological unit	Pv112, Volcanic Plain, very gently sloping (1-3%) with very low dunes
Slope	Very gently sloping (1-3%)
Micro-topography	Low hummocks (20-40cm)
Vegetation	Degraded Thorn Acacia savannah (40-80% grass cover) with low scattered shrubs (*Acacia spp.*).
Land use	Extensive grazing by Maasai and isolated small farms (remnants of the Marula Settlement Scheme).

B) General information on the soil profile.

Classification (WRB)	Areno-VitricAndosols (Dystric)
Parent material	Longonot ash (Lp8) and Akira pumice (Lpa).
Drainage class	Somewhat excessively drained
Internal drainage	Never saturated, well drained.
External drainage	Neither receiving nor shedding water.
Depth of ground water table	Below 1.50 meter.
Surface stones	None
Rock outcrops	None
Evidence of erosion	Sand deposition
Human influence	Vegetation strongly degraded due to overgrazing.

C) Soil profile description

Photo	Ho-rizon	Depth (cm)	Description
	Bw	0-47	Olive brown (2.5Y4/3) when dry loamy sand; weak to moderate, fine to medium subangular blocky; soft when dry, non sticky and slightly plastic when wet; many very fine, interstitial pores; very few fine and few very fine roots; pH 5.
	C	47-76	Dark greyish brown (2.5Y4/2) when dry loamy sand; weak, fine sub angular blocky; soft when dry, non sticky and non plastic when wet; many very fine, interstitial pores; very few very fine roots; pH 6.5.
	2C	76-81	Greyish brown (2.5Y5/2) when dry, gravely sandy clay; non sticky and non plastic; abundant medium gravel and common fine gravel, both angular shape and fresh or slightly weathered (Akira) pumice; few very fine roots.
	3C	81-104	Light yellowish brown (2.5Y6/4) when dry, gravely sandy clay; non-sticky and non-plastic; abundant medium gravel and very few coarse gravel, both angular shape and fresh or slightly weathered (Akira) pumice.
	4Bb	104-150+	Dark yellowish brown (10YR4/4) when dry sandy loam; very weak, medium to fine massive structure; soft when dry, non sticky and non plastic when wet; many very fine, interstitial pores; very few very fine roots; pH 8.

D) Laboratory data: Not available

Soil profile NAIV/2000/AN/005

A) Information on soil profile site.

Date of examination	1st October 2000.
Authors	Hennemann G.R., Nagelhout A.
Location	219745, 9903738 (UTM, ARC1960) Longonot, Naivasha area.
Elevation	2,138 meter above sea level.
Geopedological unit	Lf312, Step-faulted Plateau, lower glacis
Slope	Gently undulating (2-5%)
Micro-topography	Nearly level
Vegetation	Savannah-grassland (40-80% cover)
Land use	Extensive grazing and isolated small farms.

A. General information on the soil profile.

Classification (WRB)	Areno-VitricAndosols (Dystric)
Parent material	Longonot ash (Lp8) and Akira pumice (Lpa).
Drainage class	Somewhat excessively drained
Internal drainage	Never saturated, well drained.
External drainage	Neither receiving nor shedding water.
Depth of ground water table	Below 1.00 meter.
Surface stones	None
Rock outcrops	None
Evidence of erosion	No
Human influence	Vegetation strongly disturbed due to overgrazing.

C) Soil profile description

Photo	Ho-rizon	Depth (cm)	Description
None	Bw	0-40	Dark greyish brown (10YR4/2) when dry and very dark greyish brown (10YR3/2) when moist, loamy sand; weak to moderate, medium to fine sub angular blocky; soft when dry, non sticky and slightly plastic when wet; many very fine, interstitial pores; few very fine and very few fine roots; pH 4.5
	BC	40-61	Olive grey (5Y5/2) when dry and very dark greyish brown (2.5Y3/2) when moist, loamy sand; weak to very weak, medium to fine sub angular blocky; soft when dry; non sticky and non plastic when wet; many very fine, interstitial pores; few very fine and very few fine roots; pH 5
	C	61-92	Grey (5Y6/1) when dry and olive grey (5Y4/2) when moist sand; very weak, medium to fine sub angular blocky; soft to slightly hard when dry; non sticky and non plastic when wet; many very fine, interstitial pores; very few very fine roots; pH 5.0
	2C	92-95+	A pumice layer, greyish brown (2.5Y5/2) when dry, sandy clay; non sticky and non plastic; abundant medium gravel and common fine gravel, both angular shape and fresh or slightly weathered (pumice); few very fine roots

D) Laboratory data: Not available

Soil profile NAIV/2000/AN/006

A) Information on soil profile site.

Date of examination	1st October 2000.
Authors	Hennemann G.R., Nagelhout A.
Location	219083, 9904577 (UTM, ARC1960). Longonot, Naivasha area.
Elevation	2,124 meter above sea level.
Geopedological unit	Pv112, Volcanic Plain, very gently sloping (0-3%) with low dunes
Slope	Gently undulating (2-5%).
Micro-topography	Very low dunes (20-40 cm).
Vegetation	Savannah-grassland (40-80% cover).
Land use	Extensive grazing and isolated small farms.

B) General information on the soil profile.

Classification (WRB)	Areno-VitricAndosols (Dystric)
Parent material	Longonot ash (Lp8) and Akira pumice (Lpa).
Drainage class	Somewhat excessively drained
Internal drainage	Never saturated, well drained.
External drainage	Neither receiving nor shedding water.
Depth of ground water table	Below 1.00 meter.
Surface stones	None
Rock outcrops	None
Evidence of erosion	Slight sand deposition
Human influence	Vegetation strongly degraded due to overgrazing.

C) Soil profile description

Photo	**Hori-zon**	**Depth (cm)**	**Description**
None	Bw	0-35	Very dark greyish brown (2.5Y3/2) when dry, loamy sand; weak to moderate, medium to coarse subangular blocky; soft to slightly hard when dry; non sticky and slightly plastic when wet; many very fine, interstitial pores; few very fine and very few fine roots; pH 4.5
	C	35-55	Dark olive grey (5Y3/2) when dry, loamy sand; weak, medium to coarse subangular blocky; soft when dry; non sticky and slightly plastic when wet; many very fine, interstitial pores; very few very fine roots; pH 5
	2C	55-95	A pumice layer, greyish brown (2.5Y5/2) when dry, sandy clay; non sticky and non plastic; abundant medium gravel and common fine gravel, both angular shape and fresh or slightly weathered (pumice); few very fine roots
	3Bbw	95-100+	Very dark brown (10YR2/2) when dry, sandy loam; weak, coarse subangular blocky; slightly hard when dry; slightly sticky and slightly plastic when wet; many very fine, interstitial pores; few very fine roots; pH 9; audible reaction to HCl.

D) Laboratory data: Not available

Soil profile NAIV/2000/AN/007

A) Information on soil profile site.

Date of examination	1st October 2000.
Authors	Hennemann G.R., Nagelhout A.
Location	219939, 9902938 (UTM, ARC1960). Longonot, Naivasha area.
Elevation	2,133 meter above sea level.
Geopedological unit	Pv111, Volcanic Plain, very gently sloping (1-3%)
Slope	Very gently sloping (1-3%)
Micro-topography	Very low dunes (20-40cm)
Vegetation	Savannah-grassland (40-80% cover)
Land use	Extensive grazing and isolated small farms.

B) General information on the soil profile.

Classification (WRB)	Areno-VitricAndosols (Dystric)
Parent material	Longonot ash (Lp8) and Akira pumice (Lpa).
Drainage class	Somewhat excessively drained (S).
Internal drainage	Never saturated, well drained.
External drainage	Neither receiving nor shedding water.
Depth of ground water table	Below 0.90 meter.
Surface stones	None
Rock outcrops	None
Evidence of erosion	On the site, slight evidence of sand deposition; nearby a very deep deflation trench.
Human influence	Vegetation strongly degraded due to overgrazing.

C) Soil profile description

Photo	**Ho-rizon**	**Depth (cm)**	**Description**
None	Bw	0-61	Dark greyish brown (10YR4/2) when dry and very dark brown (10YR2/2) when moist, loamy sand; weak to moderate, coarse to medium subangular blocky; soft to slightly hard when dry; non sticky and slightly plastic when wet; very few fine angular gravel, strongly weath-ered (pumice); very few fine interstitial pores; few very fine and very few fine roots; pH 4.5
	C	61-90+	Pale olive (5Y6/3) when dry and olive grey (5Y4/2) when moist, loamy sand; weak, coarse to medium suban-gular blocky; soft when dry; non sticky and non plastic when wet; ; very few fine angular gravel, strongly weath-ered (pumice); very few fine interstitial pores; very few very fine roots; pH 5

D) Laboratory data: Not available

Soil profile NAIV/2000/AN/008

A) Information on soil profile site.

Date of examination	1st October 2000.
Authors	Hennemann G.R., Nagelhout A.
Location	219466, 9902824 (UTM, ARC1960).
	Longonot, Naivasha area.
Elevation	2,129 meter above sea level.
Geopedological unit	Pv112, Volcanic Plain, very gently sloping (0-3%)
Slope	Volcanic Plain, very gently sloping (0-3%)
Micro-topography	Level, sand deposition
Vegetation	None.
Land use	None.

B) General information on the soil profile.

Classification (WRB)	Areno-VitricAndosols (Dystric)
Parent material	Longonot ash (Lp8) and Akira pumice (Lpa).
Drainage class	Somewhat excessively drained
Internal drainage	Never saturated, well drained.
External drainage	Neither receiving nor shedding water.
Depth of ground water table	Below 1.00 meter.
Surface stones	None
Rock outcrops	None
Evidence of erosion	Very severe wind erosion, an extensive wind deposition area
Human influence	Vegetation strongly degraded due to overgrazing and sand deposition

C) Soil profile description

Photo	Horizon	Depth (cm)	Description
 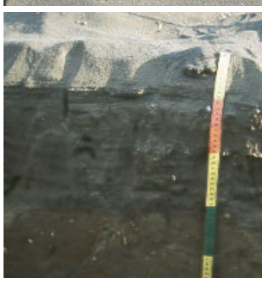	Bs1	0-23	Very dark greyish brown (2.5Y3/2) when dry, coarse and medium sand deposition; laminar; non sticky and non plastic; pH 4.5; recent sand deposition
	Bs2	23-42	Very dark grey (2.5Y3/1) when moist, coarse and medium sand deposition; laminar; non sticky and non plastic; pH 4.5; sub-recent sand deposition
	Bw	42-66	Very dark greyish brown (10YR3/2) when moist, loamy sand; very friable when moist; non sticky and slightly plastic when wet; many very fine interstitial pores; very few very fine and fine roots; pH 4.5
	C	66-87	Dark olive grey (5Y3/2) when moist, sand; weak, coarse to medium subangular blocky; loose to very friable when moist, non sticky and non plastic when wet; many very fine interstitial pores; very few very fine roots; pH 5
	2C	87-102+	Olive grey (5Y4/2) when moist, loamy fine sand; weak, coarse to medium subangular blocky; loose to very friable when moist; non sticky and slightly plastic when wet; many very fine interstitial pores; very few very fine roots; pH 6.5

D) Laboratory data: Not available

Soil profile NAIV/2000/AN/009

A) Information on soil profile site.

Date of examination	1st October 2000.
Authors	Hennemann G.R., Nagelhout A.
Location	218576, 9904439 (UTM, ARC1960). Longonot, Naivasha area.
Elevation	2,111 meter above sea level.
Geopedological unit	Pv112, Volcanic Plain, very gently sloping (0-3%), with very low dunes
Slope	Very gently sloping (0-3%)
Micro-topography	Unspecified
Vegetation	Savannah-grassland (40-80% cover)
Land use	Extensive grazing and isolated small farms.

B) General information on the soil profile.

Classification (WRB)	Areno-VitricAndosols (Dystric)
Parent material	Longonot ash (Lp8) and Akira pumice (Lpa).
Drainage class	Somewhat excessively drained
Internal drainage	Never saturated, well drained.
External drainage	Neither receiving nor shedding water.
Depth of ground water table	Below 1.00 meter.
Surface stones	None
Rock outcrops	None
Evidence of erosion	Slight evidence of sand deposition
Human influence	Vegetation strongly degraded due to overgrazing.

C) Soil profile description

Photo	**Ho-rizon**	**Depth (cm)**	**Description**
None	Bw1	0-30	Very dark greyish brown (10YR3/2) when moist, loamy sand; weak to moderate, medium subangular blocky; soft to slightly hard when dry; non sticky and slightly plastic when wet; common very fine and very few fine interstitial pores; pH 4.5
	Bw2	30-54	Very dark greyish brown (10YR3/2) when moist, loamy sand; weak to moderate, medium to fine subangular blocky; soft when dry; non sticky and non plastic when wet; common very fine and very few fine interstitial pores; pH 6.5
	BC	54-81	Greyish brown (2.5Y5/2) when dry and very dark grey when moist, loamy sand; weak, medium to coarse subangular blocky; soft when dry; non sticky and non plastic when wet; few very fine and very few fine interstitial pores; pH 8; slightly audible reaction to HCl.
	C	81-100+	Light olive grey (5Y6/2) when dry and dark olive grey (5Y3/2) when moist, loamy very fine sand; weak, coarse to medium, subangular blocky; soft to loose when dry; non sticky and slightly plastic when wet; very few very fine interstitial pores; pH 8; clearly audible reaction to HCl

D) Laboratory data: Not available

Annex 2

Oblique flight planning

Cel		*Oblique*	*Formula*
C2	Focal length	35	
C3	Negative width (mm) (along track)	36	
C4	View angle degrees (along track)	54	2*ATAN(C4*0.5/C3)*180/PI()
C5	Negative height (mm) (across track)	24	
C6	View angle degrees (across track)	38	2*ATAN(C6*0.5/C3)*180/PI()
C8	Depression angle (deg)	90	
C9	Flying height (m)	700	
C10	Flying height (feet)	2,300	C9/0.3048
C11	Terrain elevation (feet)	6,955	2120/0.3048
C12	Flight Altitude (feet)	9,255	C11+C10
C13	Stand off (centre) (m)	0	C9*TAN((90-C8)*PI()/180)
C14	Coverage (centre) (m)	480	(C4/C3)*(C9^2+C13^2)^0.5
C15	Scale centre	20,000	C14*1000/C4
C16	Ground speed knots	80	
C17	Ground speed (m/s)	48	C16*0.515
C18	Overlap required (along centre) (%)	47	
C19	Forward Gain (along centre) (m)	288	(1-(C18/100))*C14
	Time interval (seconds)	6.99	C19/C17